

Intrinsic limits to gene regulation by global crosstalk

Tamar Friedlander, Roshan Prizak, Călin C. Guet, Nicholas H. Barton, Gašper Tkačik
Institute of Science and Technology Austria, Am Campus 1, A-3400 Klosterneuburg, Austria

(Dated: June 11, 2022)

Gene regulation relies on the specificity of transcription factor (TF) – DNA interactions. In equilibrium, limited specificity may lead to crosstalk: a regulatory state in which a gene is either incorrectly activated due to noncognate TF-DNA interactions or remains erroneously inactive. We present a tractable biophysical model of global crosstalk, where many genes are simultaneously regulated by many TFs. We show that in the simplest regulatory scenario, a lower bound on crosstalk severity can be analytically derived solely from the number of (co)regulated genes and a suitable parameter that describes binding site similarity. Estimates show that crosstalk could present a significant challenge for organisms with low-specificity TFs, such as metazoans, unless they use appropriate regulation schemes. Strong cooperativity substantially decreases crosstalk, while joint regulation by activators and repressors, surprisingly, does not; moreover, certain microscopic details about promoter architecture emerge as globally important determinants of crosstalk strength. Our results suggest that crosstalk imposes a new type of global constraint on the functioning and evolution of regulatory networks, which is qualitatively distinct from the known constraints acting at the level of individual gene regulatory elements.

Life depends on the specificity of molecular recognition to ensure that essential reactions only occur between cognate substrates even when similar noncognate substrates are present, sometimes in large excess. A paradigmatic example is that of the aminoacyl tRNA synthetase [1], which uses kinetic proofreading [2] to load the appropriate amino acids onto the correct tRNAs. This and other examples—including DNA replication, ligand sensing [3], protein-protein interactions [4–9], recognition events in the immune system [10, 11], molecular self-assembly [12]—indicate that biology places a large premium on the reduction of unintended “crosstalk,” a generic term that encompasses all potentially disruptive processes occurring due to reactions between noncognate substrates.

Molecular recognition is fundamental also to transcriptional regulation, the primary mechanism by which cells control the expression levels of their genes. The specificity of this regulation ultimately originates in the binding interactions between special regulatory proteins, called transcription factors (TFs), and short regulatory sequences on the DNA, called binding sites. Although each type of TF preferentially binds certain regulatory DNA sequences, a large body of evidence shows that this binding specificity is limited, and that TFs bind other noncognate targets as well [13–17]. This suggests that the crosstalk problem is global: as the regulatory system grows in complexity, the number of potential noncognate interactions will grow faster than the number of cognate interactions. While this makes the problem biologically relevant and theoretically interesting, existing work has mostly considered a reduced setting, by computing binding probabilities for an isolated TF to cognate vs noncognate sites [18, 19]. Motivated by this observation, our primary goal here is to develop a new framework for crosstalk that captures its global nature, by treating the simultaneous problem of multiple TFs and multiple binding sites. Moreover, the focus of prior work has been

on how to achieve reliable gene regulation by cognate TFs [20], while the complementary question of how to prevent erroneous regulation by noncognate TFs has remained largely unexplored (but see [21]). As a result, it remains unclear whether crosstalk places strong constraints on the ability of cells to orchestrate their gene expression programs, and to what extent different molecular mechanisms could relax any such constraints.

To address these questions quantitatively, we construct a model of crosstalk in transcriptional regulation that satisfies three key requirements for biophysical plausibility. First, the model should be global. Global models, where many targets are simultaneously regulated by different TFs, will properly capture the faster-than-linear growth in the number of possible noncognate interactions as the number of TFs increases, and the difficulty in ensuring that recognition sequences for all TFs remain sufficiently distinct. Second, the model should explicitly account for differential activation of genes depending on regulatory conditions. Consequently—and in contrast to previously studied cases of molecular recognition [2]—the distinction between “erroneous” and “correct” outcomes of regulation will depend on the presence / absence of the regulatory signals. In particular, the ability of the regulatory system to keep genes reliably inactive when appropriate, despite crosstalk interference, will emerge as an important consideration. Third, textbook models of transcriptional regulation assume that TF-DNA interactions happen in equilibrium [19, 22]. This assumption, which is supported experimentally for prokaryotic regulation [23, 24] and which underlies the majority of modeling and bioinformatic applications, puts strong constraints on models of crosstalk. In this work, we explore its consequences in depth; we report on out-of-equilibrium schemes elsewhere [25].

Using our biophysical model we identify the parameters that have a major influence on crosstalk severity. While some of these parameters, such as the free con-

centration of TFs, are difficult to estimate, we show that there exists a lower bound to crosstalk with respect to these parameters. This lower bound is easily computable: analytically for simple regulatory schemes, and numerically otherwise. This allows us to ask a number of fundamental questions: How does the severity of crosstalk depend on the number of (co-expressed) genes or the biophysical properties of TF-DNA interactions, such as binding site length and binding energy, for which we have reliable estimates? How do the regulatory strategies of prokaryotes compare to those of eukaryotes? Do complex regulatory schemes, such as combinatorial regulation by activators and repressors, or cooperative activation, lower crosstalk, as is often implied [20]?

Many biophysical constraints have been shown to shape the properties of genetic regulatory networks, e.g., programmability [18], response speed [26], noise in gene expression and dynamic range of regulation [27–30], robustness [31], and evolvability of the regulatory sequences [32, 33]. Most of these constraints, however, could be understood at the level of individual genetic regulatory elements. Crosstalk, as analyzed here, is special: while it originates locally due to biophysical limits to molecular recognition, its cumulative effect only emerges globally. At the level of a single genetic regulatory element, crosstalk can always be avoided by increasing the concentration of cognate TFs or introducing multiple binding sites in the promoter. It is only when we self-consistently consider that these same cognate TFs act as noncognate TFs for other genes, or that new binding sites in the promoter drastically increase the number of noncognate binding configurations, that crosstalk constraints become clear.

I. RESULTS

A. A thermodynamic model of global crosstalk

We start with a thermodynamic model of regulation [23, 34], which postulates that the gene expression level depends on the equilibrium occupancy of TFs at the regulatory sites on the DNA. This model has been widely used to predict gene expression and has been experimentally validated in various systems [35–37]. We consider a cell that contains M genes, which need to be transcriptionally regulated. In the basic scenario (extended later to more elaborate regulatory schemes), each gene is associated with a single binding site of length L . The cell contains T different types of transcription factors (but not all of them are present at any given time), each regulating $\Theta = M/T$ genes. We start with the simplest setup, where there is a unique kind of TF for every gene, which (if present) preferably binds to that gene's binding site to activate transcription. In this setup, $\Theta = 1$ and thus $T = M$; we will generalize the results to $\Theta > 1$ later. Every TF can also bind other (noncognate) binding sites, albeit with lower probability, as schematized in

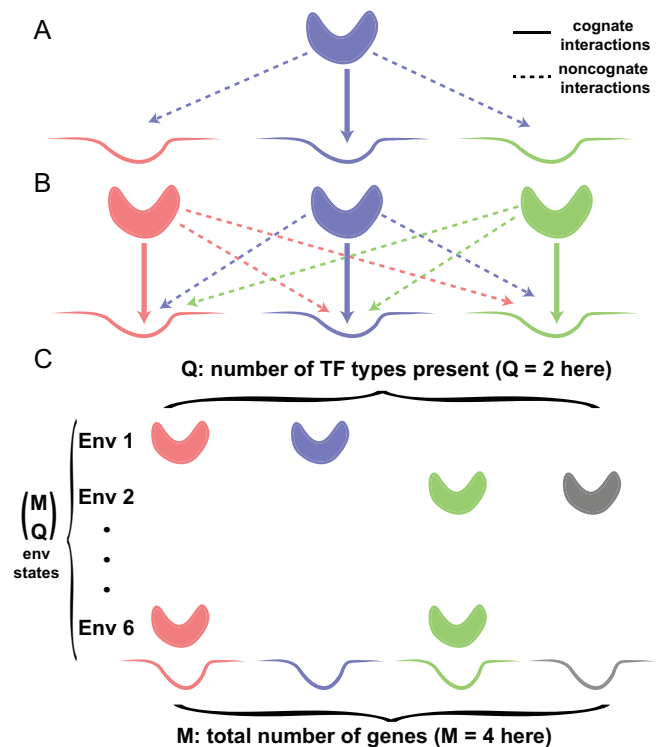


FIG. 1. **Crosstalk in gene regulation.** (A) A TF preferentially binds to its cognate binding site, but can also bind noncognate sites, potentially causing crosstalk—an erroneous activation or repression of a gene. (B) In a global setting where many TFs regulate many genes, the number of possible noncognate interactions grows quickly with the number of TFs; additionally, it may become difficult to keep TF recognition sequences sufficiently distinct from each other. (C) Cells respond to changing environments by attempting to activate subsets of their genes. In this example, the total number of genes is $M = 4$, and different environments (here, 6 in total) call for activation of subsets with $Q = 2$ genes. To control the expression in every environment, TFs for Q required genes are present, while the TFs for the remaining $M - Q$ genes are absent. Because of crosstalk, TFs can bind noncognate sites, generating a pattern of gene expression that can differ from the one required.

Figs 1A, B. These noncognate interactions contribute to crosstalk in our model.

The binding probability of a TF to any binding site is determined by two factors: the effective concentration of TFs, and the binding energy. For now, we leave the concentration as a free parameter that reflects the number of freely diffusing TFs in the cytoplasm, as well as any possible effects due to nonspecific TF localization on the DNA or elsewhere [38]. We assume that the binding energy only depends on the number of mismatches between a particular binding site and the consensus sequence unique to the given TF. Each binding site can thus exist in either of the three possible states [34]: (i), bound by a cognate TF; (ii), bound by a noncognate TF; or (iii), unbound. Energetically (i) is the most favor-

able state and is assigned the energy $E = 0$. The unbound state (iii) is usually energetically least favorable with energy $E_a > 0$. Between these two extremes there exists an “energy ladder” of noncognate-bound configurations (ii) whose energy scales linearly with the number of nucleotide mismatches (Hamming distance) d , i.e., $E(d) = \epsilon d$. This mismatch energy model provides a tractable approximation to more detailed models [24], and has been extensively used in the literature [18, 39].

Gene regulation gives cells the ability to differentially activate subsets of their genes in a manner appropriate to the environmental conditions, signals, cell type, or time. In our simplified model, we imagine a cell that responds to different environments by activating different subsets of Q genes (out of a total of M genes), while keeping the remaining $M - Q$ genes inactive (see Fig 1C). As regulation unfolds, the regulatory network thus switches between equilibrium states where any choice of Q out of M genes could be activated; to make the problem tractable, we assume that all these choices are equiprobable. In a given environment, activating a particular subset of Q out of M genes is achieved by having the Q TF types, associated with these Q genes, present at nonzero concentration; the remaining $M - Q$ transcription factor types, corresponding to the genes that should remain inactive, will have zero concentration. Crosstalk occurs because of nonzero probability that TFs will erroneously control noncognate genes due to limited specificity, even if their presence and concentrations were adjusted perfectly to the environment. Because we will ultimately be interested in the lower bound on crosstalk error, we will assume such perfect adjustment; as a result, we will not need to specify the mechanism by which cells express the required subset of TF types or tune their concentrations in a manner appropriate to the environment. Biologically, such processes likely involve complex regulatory network dynamics with feedback loops, but since these are also affected by crosstalk it is unclear whether they could feasibly lead to improvement relative to the optimal scenario considered here.

In this model, the crosstalk error can be separated into two contributions that can be computed using basic statistical mechanics:

1. For a gene i that should be **active** and whose **cognate TF is therefore present**, error occurs if its binding site is bound by a noncognate regulator (activation out of context due to crosstalk), or if the binding site is unbound (gene is inactive). This happens with probability

$$x_1(i) = \frac{e^{-E_a} + \sum_{j \neq i} C_j e^{-\epsilon d_{ij}}}{C_i + e^{-E_a} + \sum_{j \neq i} C_j e^{-\epsilon d_{ij}}}, \quad (1)$$

where C_j is the concentration of the j th TF, d_{ij} is the number of mismatches between the j th TF consensus sequence and the binding site of gene i , and ϵ the energy per mismatch; all energies are measured in units of $k_B T$.

2. For a gene i that should be **inactive** and whose **cognate TF is therefore absent**, crosstalk error only happens if its binding site is bound by a noncognate regulator (erroneous activation) rather than remaining unbound. This happens with probability

$$x_2(i) = \frac{\sum_{j \neq i} C_j e^{-\epsilon d_{ij}}}{e^{-E_a} + \sum_{j \neq i} C_j e^{-\epsilon d_{ij}}}. \quad (2)$$

There exist other reasonable definitions of crosstalk, one of which we tested and found our results robust to the alternative formulation (SI Appendix).

We proceed by assuming full symmetry between TF concentrations (i.e., $C_j = C/Q$, where C is the total concentration of all regulators), nonspecific binding sites, and relative contributions to crosstalk error, and later show how these assumptions can be relaxed. Given that a fraction of Q/M genes have crosstalk probabilities x_1 and a fraction $1 - Q/M$ have a crosstalk of x_2 , it is easy to show that the expected fraction of genes experiencing crosstalk is simply

$$X = \frac{Q}{M} x_1 + \frac{M - Q}{M} x_2, \quad (3)$$

where we averaged over all possible subsets of Q out of the total of M genes, representing the various environments to which the cell needs to respond (see SI Appendix for calculation). X ranges between zero (no erroneous regulation) and one (every gene is mis-regulated).

The remaining step requires us to compute the partition weight of all noncognate configurations, $\sum_j C_j e^{-\epsilon d_{ij}}$, which appears in Eqs (1, 2). In a fully symmetric setup with many genes and $Q \gg 1$ we can write

$$\sum_j C_j e^{-\epsilon d_{ij}} \approx \frac{C}{Q} Q \sum_d P(d) e^{-\epsilon d} \equiv CS(\epsilon, L), \quad (4)$$

where $P(d)$ is the distribution of mismatch distances between all pairs of binding sites in our model. Equation (S9) defines $S(\epsilon, L)$, the average binding site similarity. S is proportional to the probability of a TF to bind *any* binding site. At one extreme, if all sites are identical ($d = 0$), $S = 1$; at the other extreme, when $\epsilon d \gg 1$ or $P(d) = 0$ for sufficiently large $d_{\min} \leq d$, the sites are effectively different and $S \rightarrow 0$. Figure 2A illustrates how the binding site similarity is affected by the length of the binding site L and the mismatch energy ϵ .

The binding site similarity $S(\epsilon, L)$ of Eq (S9) can be estimated either from data directly or computationally, under certain assumptions on how binding sites are organized in sequence space. In Fig 2B we used databases of known TF binding sites to extract organism-specific estimates for S . We further considered two computational approaches. If the binding sites are random sequences of length L drawn from a uniform distribution,

i.e., the regulatory network uses a “random code” to address individual genes, S is computable analytically (see SI Appendix): $S(\epsilon, L) = \left(\frac{1}{4} + \frac{3}{4}e^{-\epsilon}\right)^L$. Alternatively, we asked about optimal sequence space packing: how to choose M sequences of length L such that each pair differs by at least some d_{\min} (see SI Appendix). This can be mapped onto an optimal code design problem [40], which is intractable in general, but approximations can be constructed numerically. A separate issue we also considered is whether the basic mismatch model of TF-DNA interaction energy needs to be made more realistic, e.g., by taking into account that the binding energy saturates to a constant after a certain number of mismatches [16]. We find that all these variations ultimately only affect the value of S while leaving the crosstalk formalism unchanged. We therefore carried out all the computations either as a function of S directly, or, where appropriate, by assuming the random code. Figs 2C, D show how values of S for the random code map to alternative models.

B. Basic crosstalk model exhibits three distinct regulatory regimes

While we can reasonably estimate the major determinants of crosstalk in our model—the number of (coactivated) genes Q and M , and the binding site similarity S —it is harder to determine the appropriate value for the total concentration of available TFs, C . This is not only due to the lack of quantitative data, but also because the relation between the total copy number of TFs in a cell and the concentration of TFs that are available for binding may be complicated. We thus opted for an alternative approach: we look for a concentration C^* that minimizes the crosstalk error X . Such a minimum, $X^* = X(C^*)$, therefore represents a lower bound on crosstalk in our basic model, introduced above and summarized in Fig 3A.

The optimization yields three distinct regulatory regimes, illustrated in Figs 3B, C. When binding sites are very similar, such that $S > 1/(M - Q)$, the error is minimized by taking $C^* = 0$, i.e., having no regulation at all (region I). The resulting value for the crosstalk is then $X^* = Q/M$, the fraction of genes that should have been active (the total error is thus solely due to x_1 contribution, while $x_2 = 0$). Interestingly, the extent of this regime increases with $M - Q$, the number of genes that must remain inactive.

There is a broad region in the (S, Q) plane where crosstalk is minimized by a finite positive value for the optimal TF concentration—we call this the “regulation regime” (region III). For small S , optimal $C^* \sim \frac{e^{-E_0}}{\sqrt{S}} \frac{Q}{\sqrt{M-Q}}$ to leading order, yielding

$$X^* = \frac{Q}{M} \left(-S(M - Q) + 2\sqrt{S(M - Q)} \right). \quad (5)$$

This simple expression for X^* is one of our key results. The crosstalk depends both on the fraction of

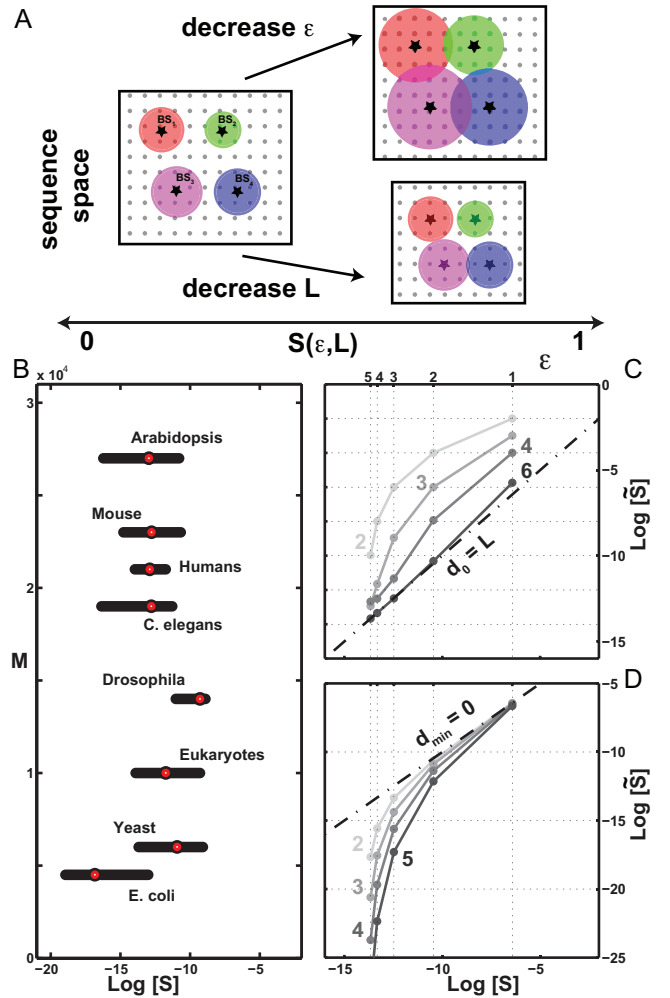


FIG. 2. **Binding site similarity S and number of genes M are basic determinants of crosstalk.** (A) Binding site similarity, $S(\epsilon, L)$, determines the likelihood that a TF will bind noncognate sites, if recognition sequences are of length L and the energy per mismatch is ϵ . A schematic diagram of sequence space packing by different TFs: sequences (dots) in a colored circle are likely to be bound by the TF whose consensus is the circle’s center. Smaller L contracts the sequence space and makes crosstalk (circle overlap) more likely (larger S); crosstalk is increased (larger S) also by smaller ϵ , which expands the circle radius. (B) Typical values for the number of genes, M , and binding site similarity, $S(\epsilon, L)$, across different taxa, estimated from genomic databases. For each organism, we find a distribution of S over its reported TFs (dots = median of the distribution, black bars = ± 1 -quartile range; see SI Appendix for details). (C, D) Alternative biophysical models lead to values for \tilde{S} (y-axis) that can be remapped to the $S(\epsilon, L)$ (x-axis) for the random code with the mismatch energy model, $E(d) = \epsilon d$ and $L = 10$ bp binding sites (corresponding scale for ϵ shown in the top axis). Dashed lines denote equality. (C) An improved affinity model where the mismatch energy saturates after d_0 mismatches, $E(d) = \epsilon \min(d, d_0)$ (gray lines = different d_0 as indicated), effectively increases S . $d_0 \sim 4$ has been reported experimentally [16]. (D) Optimally designed binding sites effectively decrease S . Here, their sequences are at least d_{\min} bp distant from each other (gray lines = different d_{\min} as indicated).

activated genes, $\frac{Q}{M}$, as well as on the total number of genes that need to be inactive, $M - Q$. If a fixed fraction $\alpha = Q/M$ genes is activated, then in the regulation regime $M < 1/((1 - \alpha) \cdot S)$. The (inverse of the) binding site similarity, $1/S$, therefore puts an upper bound on the total number of genes, M , that an organism can maintain before crosstalk disrupts the regulation. Increasing the energy gap between cognate and unbound states, E_a , only lowers the optimal concentration, while leaving the crosstalk error invariant. As Q increases towards a limiting value $Q_{\max}(S, M)$, the optimal concentration C^* increases until we reach a regime where C^* formally diverges (region II), shown in Fig 3C and Fig S1. In this limit, however, a biologically plausible solution would simply be to constitutively express the majority of the genes rather than using transcriptional regulation to do so.

One could hypothesize that the “no regulation” ($C^* = 0$) regime is an artefact of the symmetric choice of weights and that penalizing erroneous activation, i.e., expression of unnecessary proteins, equally to the incorrect expression of the necessary proteins is too harsh. To study this, we varied the relative weight of the two components (x_1, x_2) of crosstalk in Fig 4A to find that all three regimes exist generically, although their boundaries may shift. The existence of the three distinct regimes is thus not a consequence of our choice to weigh both contributions to error in Eq (3) equally.

We also extended the crosstalk model to break the symmetry between the genes: we designated a fraction h of all genes as “important”, penalizing their contribution to the total crosstalk X more severely, while allowing the TF concentrations to optimally reallocate between the important genes and the remaining ones. Figure 4B shows how the crosstalk limits behave in this case, and illustrates that the crosstalk model can be generalized to arbitrarily heterogenous setups.

We asked if regulation by repression alone leads to differences with respect to the activation scenario examined here. We find a simple mathematical symmetry that relates the crosstalk equations of the activator model to those of the repressor model (SI Appendix). In the repressor case all three regimes reported above can be identified as well, and the minimal crosstalk values are comparable to the activator case. One could consider mixed models, where activation is used for some genes and repression for the others, or where the best of the two strategies is chosen depending on parameters M, Q , and S , but we leave this for future work.

Finally, we analyze the more general formulation of the model where instead of a single gene, each TF regulates Θ genes that are assumed to have identical binding sites (if the sites are not identical, the crosstalk will only worsen). That is, the cell still contains M genes in total, out of which Q need to be activated by the appropriate presence or absence of T TF types. The achievable crosstalk is now lower (see SI Appendix for analytical expression). Interestingly, however, while the cell can only regulate

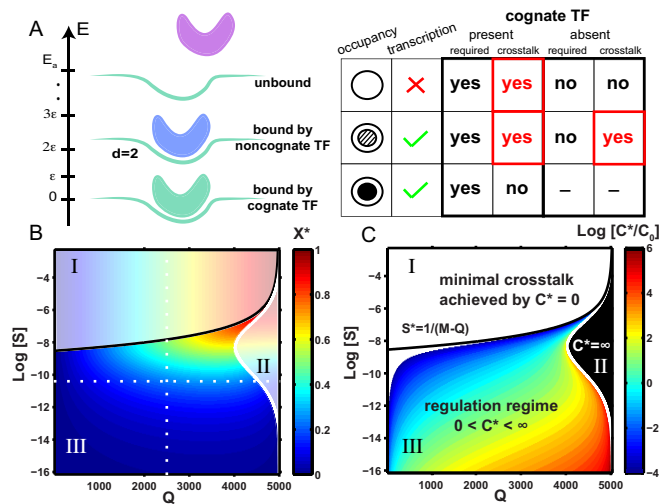


FIG. 3. Basic model with one activator binding site per gene exhibits three distinct regulatory regimes. (A) Each binding site can be in either of the three possible states with different corresponding energies: bound by a cognate factor ($E = 0$, green molecule), bound by a noncognate factor with d -mismatches ($E = \epsilon d$, here blue molecule with $d = 2$), or unbound ($E = E_a$). The table shows which of these states lead to transcription and which of these outcomes is considered as crosstalk when the cognate TF is present and the gene is required to be active (left), or absent and the gene is required to be inactive (right). (B) Minimal crosstalk X^* , shown in color, as a function of the number of coactivated genes Q and binding site similarity, S . Three different regulatory regimes are separated by black and white boundary lines (analytical expressions in SI Appendix), identical between panels (B) and (C). Dotted lines refer to the “baseline parameters” ($Q = 2500, S = 10^{-4.5}$ with $L = 10, \epsilon = 2$ and $M = 5000$) that we use in all subsequent figures if not specified differently. (C) Optimal TF concentration, C^* , that minimizes the crosstalk, relative to C_0 , the optimal concentration at baseline parameters. For high binding site similarity (large S), the crosstalk is minimized at $C^* = 0$ (white region, I: “no regulation regime”). For $Q \rightarrow M$ and intermediate S , the crosstalk is minimized at $C^* \rightarrow \infty$ (black region, II: “constitutive regime”). In a large, biologically plausible intermediate regime, crosstalk is minimized at a finite nonzero TF concentration (color, III: “regulation regime”).

sets of Θ genes, rather than being able to individually control the activity of each gene, the crosstalk and the optimal TF concentration, C^* , decrease more slowly than $1/\Theta$ (in particular, the x_1 component and to leading order C^* only decrease as $1/\sqrt{\Theta}$), showing that there is an inherent tradeoff between crosstalk and the power that the regulatory system has to exert detailed control over individual genes (see SI Appendix).

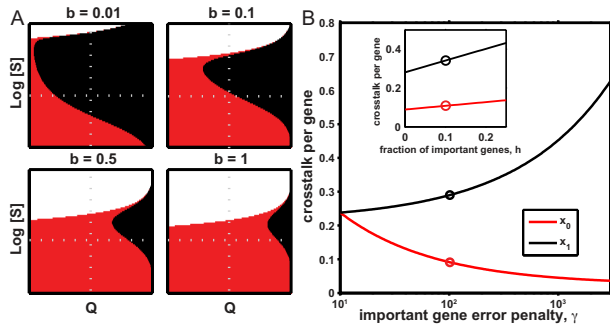


FIG. 4. **Varying relative importance of either crosstalk types or genes preserves basic model properties.** (A)

To break the symmetry between the two error types we consider a redefined crosstalk, $X(b) = \frac{Q}{M}x_1 + b\frac{M-Q}{M}x_2$ ($b = 1$ for the basic model of Eq (3)). For different values of b all three regulatory regimes are preserved, although their boundaries shift. Red shows the “regulation regime,” ($0 < C^* < \infty$). As erroneous activation is penalized less (decreasing b), the “no regulation” ($C^* = 0$, white) regime shrinks, whereas the constitutive expression regime ($C^* = \infty$, black) expands, as expected. (B) To break the symmetry between genes, we define a fraction h (out of Q) genes as important, having γ -times higher contribution to the total crosstalk. TF concentration for these genes is optimized separately, subject to the total TF concentration C remaining fixed to its optimal value in the symmetric, $\gamma = 1$, case. We show the crosstalk per important gene, x_0 (red), and per a normal gene, x_1 (black), as a function of γ (for $h = 0.1$). The inset shows the same as a function of h (for $\gamma = 10$). Per-gene crosstalk increases approximately linearly with h and important genes achieve $\sim \sqrt{\gamma}$ smaller crosstalk relative to normal genes.

C. Cooperativity reduces crosstalk and the required optimal TF concentrations

Cooperativity, a commonly observed transcriptional regulatory mechanism, refers to molecular configurations where the binding of multiple TF molecules is energetically favored beyond the individual affinity for their binding sites. Cooperativity has been studied for its dynamical properties and the role of increasing specificity [20, 41]; here we examined its ability to alleviate crosstalk. We extended our gene regulation model such that each gene is now influenced by two nearby binding sites of length L to which cognate TFs can bind cooperatively. For simplicity we assume that cooperativity occurs between TFs of the same type, although the framework can be extended to more general cases. This molecular configuration of two cognate DNA-bound proteins is favored by an additional energy contribution Δ (for the full list of thermodynamic configurations and the calculation of crosstalk see SI Appendix). Only one of the two sites controls transcriptional activity directly

(here, the site proximal to the gene start, e.g., by polymerase recruitment [23]), while the other – here, the distal site – helps stabilize the binding to the proximal site, as schematized in Fig 5A. In the limit $\Delta = 0$, the distal binding site has no effect on regulation, and this case reduces to the basic model of regulation by a single binding site (Fig 3).

To assess whether cooperative regulation can reduce the crosstalk, we computed the minimal achievable crosstalk, X_{coop}^* (by numerically optimizing over TF concentrations C and cooperativity energy Δ), and compared this in Fig 5B with the minimal crosstalk of the basic model, X^* . We find that cooperativity can significantly reduce crosstalk in a large part of the “regulation regime,” which itself extends towards larger S . Examining in detail how the crosstalk behaves as a function of Δ and L in Fig 5C, we see that at a fixed binding site length L , minimization of crosstalk prefers strong cooperativity; nevertheless, the improvement in crosstalk is bounded and as Δ grows, saturates at a limiting value. Increasing Δ does, however, lead to a smaller required concentration of the regulators. These changes are apparent in Fig 5D that shows the optimal concentrations achieving the minimal error as a function of L and Δ . In this scenario, as Δ grows, crosstalk can approach and even drop below the crosstalk of the basic model with a binding site which is twice as long. This is a relevant comparison because the cooperative regulation does, in fact, have access to a total of $2L$ base pairs of recognition sequence. Nevertheless, cooperative regulation is not fully equivalent to this case. While the cooperative scheme has access to $2L$ bp, the two sites are constrained to be identical, making the effective sequence space only as large as that of a single site of length L .

The cooperative model presented here assumed that cooperative interaction between two TF molecules can only occur when they bind their cognate binding sites. This clearly must help reduce crosstalk but requires an additional recognition mechanism and might not always be biologically plausible. If many kinds of TFs in the cell are cooperative and the stabilization energy Δ comes from protein-protein interactions, one would imagine that two TFs of the same type—thus able to interact and gain the cooperative benefit—could cause erroneous activation upon binding to noncognate sites. While this configuration is suppressed relative to cognate binding by mismatch energy penalty from two noncognate TFs, there are $Q - 1$ same-type noncognate TF pairs, and only one cognate pair, per gene. We studied this model variant in the SI Appendix and found that, indeed, when binding sites are too similar ($\log(S) \gtrsim -6$), allowing “noncognate cooperativity” drastically increases the crosstalk error (e.g., ~ 2 -fold, from roughly 0.15 to 0.30, at $\log(S) = -6$ and $Q = 2500$; at baseline parameters, $X_{\text{coop}}^* = 0.07$ with vs. $X_{\text{coop}}^* = 0.01$ without noncognate cooperativity, as shown in Fig S6). In this case, it is also instructive to look analytically at the strong cooperativity, $\Delta \rightarrow \infty$, limit. In this limit, when the

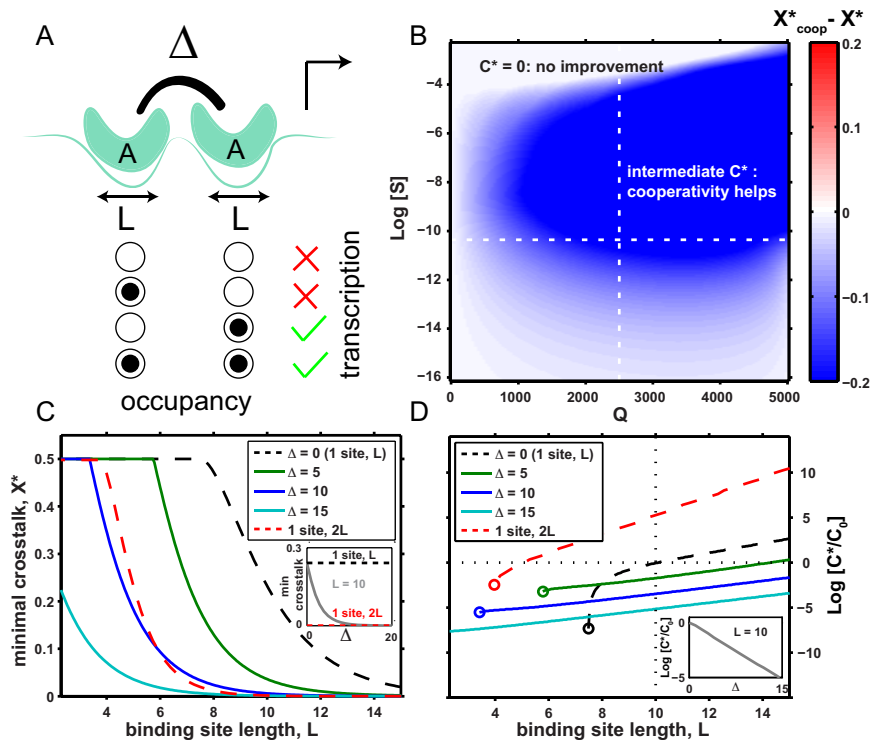


FIG. 5. **Cooperative regulation reduces crosstalk and the required optimal TF concentration.** (A) Cognate binding configurations (necognate not shown) for two sites of length L leading to transcription (green check) or not (red cross); doubly occupied promoter gains a cooperative energy Δ . Transcription proceeds only when the proximal (rightmost) site is occupied. (B) Difference in minimal crosstalk, shown in color, between the cooperative model and the basic model of Fig 3, $X_{\text{coop}}^* - X^*$. Cooperativity significantly reduces crosstalk (blue; at baseline parameters shown with white dashed lines, $X_{\text{coop}}^* = 0.01$ here vs. $X^* = 0.24$ in the basic model) and shrinks the “no regulation” ($C^* = 0$) regime. (C) Minimal crosstalk error, X^* , vs. binding site length L for different values of cooperative energy, Δ , shows that strong cooperativity can decrease the crosstalk beyond the basic model with binding site of length $2L$ (red). (D) Optimal TF concentration, C^* , required to minimize cross talk decreases with increasing cooperativity Δ for all L , and is consistently below the single-site basic model with site length of either L (black) or even $2L$ (red). Circles denote transition to the “no regulation” ($C^* = 0$) regime at low L (large S), showing that cooperativity extends the “regulation regime.”

only likely occupancy configurations on the promoter are either the empty state or doubly-occupied states, the cooperative model reduces to a new “effective” basic model after an appropriate transformation of variables (see SI Appendix): $\tilde{C} = C^2$, $\tilde{E}_a = 2E_a + \Delta$, $\tilde{S} = S(2\epsilon, L)$, such that $X_{\text{coop}}(C, S, E_a, \Delta \rightarrow \infty) = X(\tilde{C}, \tilde{E}_a, \tilde{S})$, where X is the crosstalk of the basic model given by Eq (S8). In the relevant parameter range, $S(\epsilon, 2L) < \tilde{S} = S(2\epsilon, L)$. As a consequence, two short binding sites of length L with cooperative interaction decrease crosstalk compared to a single short binding site of length L , but they are still inferior to a single binding site of length $2L$.

This case of necognate cooperativity is also relevant for a regulatory mechanism commonly present in prokaryotic regulation, where TF monomers often dimerize in solution before binding to DNA. If the two binding sites predominantly act as half-sites for the binding of a single dimer, the relevant equations for crosstalk are identical to necognate cooperativity in the large Δ limit, with C being the concentration of monomers. As a result, regulation by TF dimers is expected to reduce the

crosstalk compared to monomers as shown in Fig S6, but not to the extent possible if cooperativity were specific, as is the case for Fig 5.

The two cases of cooperativity we considered here represent two extremes of a spectrum: cooperative interaction is either possible exclusively at the cognate site, or at all sites equally. There probably exist intermediate situations which help limit the occurrence of spurious cooperative interactions. A simple example of such a mechanism could utilize the positioning of the binding sites on the DNA: only when a pair of sites is spaced by an appropriate amount are the cooperative interactions possible for the cognate TFs. If different TF types use different spacing, the harmful effects of cooperativity at a particular necognate site pair will be restricted to a subset of TFs. More complex geometrical arrangements, e.g., cooperative interactions involving DNA looping or allosteric effects between the two TFs and the DNA [42], could provide similar benefits.

The issue of cooperative interactions during necognate binding is a striking demonstration of how a seem-

ingly microscopic detail may influence global crosstalk, while it has no bearing on the aspects for which cooperativity has been studied traditionally: its ability to sharply activate the cognate gene in response to small increases in concentration. More generally, these results suggest that out of the many molecular mechanisms suggested to induce cooperativity (e.g., synergistic activation [20], nucleosome-mediated cooperativity [43], dimerization, energetic interactions on the promoter, etc.), those for which the cooperative energy is gained solely upon cognate binding can better withstand crosstalk interference.

D. Combinatorial regulation by activators and repressors has a marginal effect on crosstalk unless their parameters are specifically tuned

An important contribution to crosstalk is the erroneous activation of genes that should remain inactive. Naively, one might argue that any kind of global repression could alleviate this problem by preventing spurious transcription. A variety of mechanisms could fulfill this role, ranging from direct control by transcriptional regulators to more elaborate schemes like nuclear import/export, DNA packing onto nucleosomes, covalent modifications of DNA and histones, etc. Global repression was even suggested as having enabled several evolutionary transitions to more complex and larger genomes [21]. The simple argument for global repression, however, disregards the possibility that this repression itself causes and contributes to additional crosstalk. To explore this in detail, we extended our basic model to include an additional nonspecific repressor, such that the binding site of each gene can be bound either by activators (cognate or noncognate) or by this global repressor; in the latter case, the gene is silenced (SI Appendix). Perhaps not surprisingly, we find that the minimal achievable crosstalk error in this extended scheme is exactly the same as in the basic setup, regardless of the concentration and the affinity of the sites. The only effect of the repressor is to effectively “dilute out” the activators, making the scheme ineffective.

We next turned our attention to a sequence-specific repression mechanism. In an extension to our basic model, we equipped each gene with both an activator and a repressor site, such that each of these sites has its own cognate regulator (activator or repressor). For the Q genes that should be active, only their Q cognate activators (but not repressors) were present. For the remaining $M - Q$ genes that should be inactive only their cognate repressors (but not activators) were present. Repressor sites could have a different affinity (E_r) for TFs from the activator sites (E_a). All activators (repressors) are present at concentrations C_a (C_r), where C_a need not equal C_r ; we numerically optimized over E_r and the concentrations to find the minimal achievable crosstalk. Importantly, we considered two possible molecular ar-

rangements on the promoter: in the *non-overlapping sites* scenario (Fig 6A, left) the two binding sites could be occupied by regulatory molecules simultaneously, whereas in the *overlapping sites* scenario (Fig 6A, right), either the activator or repressor site, but not both, could simultaneously be occupied. Whether this exclusion happens because the two binding sites literally overlap or due to more complex mechanisms is not crucial for our results. We assumed that a bound repressor inactivates transcription, regardless of the activator state; for a detailed list of molecular configurations on the promoter, see SI Appendix. In the non-overlapping case, small ($\sim 10\%$ at baseline parameters) decreases in crosstalk error are nominally possible, as shown in Fig 6B. A detailed examination, however, argues against this mechanism for crosstalk reduction. Optimization in Fig 6D assigns the repressor sites a very weak, or even vanishing, affinity for the TFs, $E_r \ll E_a$: in essence, the repressor sites energetically favor staying empty to the same amount as binding a cognate repressor, to fight off noncognate binding. As a costly consequence, the optimal concentration of the required TFs needs to be larger by an unreasonable factor, ~ 10 log units, relative to the basic model, to achieve the small crosstalk reduction gain.

In contrast, the overlapping case provides a greater crosstalk reduction ($\sim 25\%$ at baseline parameters), as shown in Fig 6C. The optimal repressor sites have similar affinity to their cognate TFs as do the optimal activator sites, $E_a \approx E_r$ ($E_r = E_a$ if $Q = M/2$, see SI Appendix for other Q); the benefit of the repressors quickly vanishes if this condition is not met. The total required regulator concentration now no longer has a clearly defined optimum, but does exhibit a plateau where the crosstalk is minimized. Importantly, as shown in Fig 6E, this plateau is reached for concentrations only ~ 2 log units higher than in the baseline case, making this solution biologically plausible.

In sum, the case for combinatorial regulation by activators and repressors to reduce crosstalk is complicated. Combinatorial regulation provides a smaller absolute improvement than cooperativity, but this improvement is also centered around smaller values for binding site similarity, $\log(S) \lesssim -10$, where the crosstalk of the basic model is itself already lower. Interestingly, this gain is realistically achievable only with one of the two regulatory schemes considered, further illustrating that certain molecular details at the promoters or enhancers might have strong effects on global crosstalk.

II. DISCUSSION

Finite specificity of recognition reactions is a fact of life at the molecular scale. In transcriptional regulation, which takes place in a mix of cognate and noncognate transcription factor species, the consequences of this fact could be severe—but have surprisingly not been taken to their logical conclusion. We constructed a theoretic-

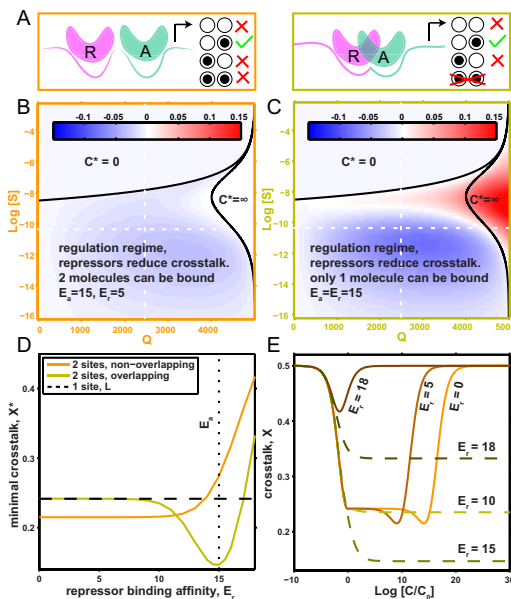


FIG. 6. Combinatorial regulation by activators and repressors yields marginal improvements in crosstalk error. (A) Separate (left) or overlapping (right) binding sites for activators A and repressors R. A subset of binding configurations for cognate regulators is shown; transcription proceeds (green) only when the A site is bound by the cognate activator and the R site is unbound. (B,C) Difference (shown in color) between minimal crosstalk achievable with activator-repressor regulation, and the basic model of Fig 3. With optimal value for the affinity of repressor sites (E_r) selected in both cases, a small overall improvement in crosstalk error is seen in (B), and a larger improvement, but localized to $\log S \lesssim -10$, in (C). At baseline parameters (white dashed lines), $X^* = 0.21$ for the non-overlapping case, $X^* = 0.18$ for the overlapping case and $X^* = 0.24$ in the basic model. (D) Dependence of the crosstalk on the repressor binding affinity E_r (activator affinity fixed at $E_a = 15$). When $E_r > E_a$, the crosstalk quickly increases: instead of helping prevent erroneous activation, repressors themselves bind too frequently in noncognate configurations, aggravating the crosstalk. For non-overlapping sites scenario, $E_r \ll E_a$ is optimal, whereas in the overlapping sites case, $E_r = E_a$ is optimal. (E) Dependence of crosstalk on the total concentration, C , of transcription factors, for non-overlapping sites case (orange-brown curves representing different E_r , as indicated) and overlapping sites case (green curves representing different E_r , as indicated). The total concentration is optimally split between activators and repressors for each C , and is reported relative to the optimal concentration C_0 of the basic model.

cal framework for crosstalk that accounts for all possible cross interactions between the regulators and their binding sites. In this global, binding-site-centered model we computed the lower bound on the probability of regulating a gene incorrectly. These limits to gene regulation, either in the basic setup with a single activator per gene or more complex setups using combinatorial regulation,

depend only on the number of total (coactivated) genes Q and M , and the binding site similarity S .

Qualitatively, these parameters robustly define three possible regulatory regimes. When binding sites are too similar to each other ($S > 1/(M - Q)$), regulation cannot prevent spurious activation of genes that should have been inactive, and “no regulation” is the best the cell can do. As Q crosses a threshold, $Q > Q_{\max}(S, M)$, cells should simply get rid of the regulatory apparatus and express all their genes, a “constitutive regime” that might be relevant for organisms that live in nearly constant environments, e.g., obligatory parasites. Finally, in the remainder of the parameter space, regulation is beneficial and there exists an optimal TF concentration, $0 < C^* < \infty$, that minimizes crosstalk.

Where do real organisms find themselves in this parameter space? Prokaryotes have very specific transcription factors, with binding site similarity estimated to be in range $-20 \lesssim \log(S) \lesssim -13$ (Fig 2A), consistent with previous reports [14]. This is deeply within the “regulation regime,” assuming typical values of $M = 5000$ and $Q \approx M/2$. In the basic model of Fig 3, the corresponding crosstalk errors would range from 10% to below 1%, and this residual crosstalk can be almost completely removed with plausible cooperativity mechanisms, e.g., via dimerization of TFs in solution.

The situation is very different for eukaryotes, where the binding site similarity is typically $-15 \lesssim \log(S) \lesssim -9$. At our baseline parameters and $M \sim 5000$, which is relevant for yeast or possibly for higher eukaryotes under the assumption that most of their genes are silenced by non-transcriptional mechanisms, the lower bound for crosstalk error stands at a very significant $X^* = 0.24$. Taking into account that real TFs have a cutoff in their binding specificity, as in Fig 2C, the typical $\log(S)$ could increase by a further 1-2 units, moving it close to the boundary of the “regulation regime” at $\log(S) = -7.8$. Considering even larger $M \sim 20000$ at $Q = M/2$ makes matters worse. The boundary of the “regulation regime” decreases to $\log(S) = -9.2$ and at our baseline parameters the crosstalk error would be an overwhelming $X^* = 0.43$, while remaining well above 10% even with considerably smaller S .

Surprisingly, quantitative analysis reveals that crosstalk constraints are not easily removed by molecular mechanisms that appear beneficial at first glance. Global repression mechanisms are ineffective, as is the combination of activation and repression unless the binding of the corresponding TFs is exclusive and binding sites are sufficiently distinct ($\log(S) \lesssim -10$). Even under these restrictive conditions, the improvements to crosstalk are marginal. Cooperativity, in contrast, seems to perform better and also requires lower TF concentrations. Most of this gain, however, is lost if cooperativity is itself not specific, i.e., if noncognate TFs of the same type can also bind cooperatively, as is likely the case with many documented molecular mechanisms. For example, eukaryotes with $M = 20000$ genes using a

cooperative scheme could reduce the crosstalk error to $X^* = 0.15$ at baseline parameters. While this is a large decrease from $X^* = 0.43$, it still represents a significant amount of erroneous regulation.

Our results lead to two general conclusions. First, various schemes of molecular control logic at promoters and enhancers [44], while nearly equivalent in the absence of crosstalk, can behave very differently in the presence of noncognate regulators [45]. Thus, molecular details such as whether noncognate TFs can bind cooperatively or not, and whether activator and repressor TF binding is exclusive or not, seem to make a large difference for global crosstalk. This highlights the need to further understand signal processing at complex promoters [46], and calls for experimental measurements of crosstalk in various regulatory architectures. Previous work in bacteria attempted to explain the preferential use of certain regulatory schemes due to their measured resilience to crosstalk [47]. Direct measurements of crosstalk, however, are challenging precisely because crosstalk is a global effect and experimentally influencing noncognate binding in a controlled manner appears difficult. An alternative approach would be to search for indirect signatures of crosstalk. A promising line of research supported by a large body of recent experimental evidence would be to examine “pervasive transcription” in eukaryotes [15, 48] as a proxy for erroneous initiation, perhaps due to crosstalk interference.

Our second conclusion is that global crosstalk represents a strong constraint in eukaryotic regulation that can be mitigated, but not easily removed. Clearly, this conclusion is based on a greatly simplified model of gene regulation. We addressed some of the restrictions of our model by breaking the symmetry between genes and crosstalk types, while others, e.g., the operon organization in prokaryotes or the accessibility of regulatory sequence in eukaryotes, could be treated by adjusting the effective Q and M ; we also considered cases where each TF regulates a subset of genes. These variations, however, do not relax crosstalk constraints significantly.

This is because the major determinant of crosstalk is the strong limit imposed by the observed values of the binding site similarity S , which primarily depends on the typical mismatch energy ϵ and the length of the binding sites, L . The scale of the mismatch energy is set by the energetics of hydrogen bonds to $\sim 2 - 4k_B T$, while the length of individual binding sites appears strongly constrained by evolutionary considerations to ~ 10 bp [49, 50], limiting the performance of our basic, single-site model.

Why, however, do complex regulatory schemes with multiple sites only yield such limited decreases in crosstalk? The answer is twofold. Complex schemes lead to an explosion of possible noncognate configurations. Furthermore, any equilibrium scheme, no matter how complex, faces a fundamental limit to its achievable error, for reasons that led Hopfield to propose kinetic proofreading [2]. Decreases in crosstalk that we observed are thus likely due to the ability of the complex schemes to effectively “read out” a longer recognition sequence (i.e., effectively decreasing S), but the residual crosstalk for a typical eukaryote appears substantial. It remains to be seen if such considerations place an upper bound on the number of possible transcription factors [40], or if they ultimately limit the complexity of simpler regulatory networks to the point where completely new mechanisms must have evolved, for instance, gene silencing, localization of transcriptional activity, or regulation by molecular reaction schemes out of equilibrium [25].

ACKNOWLEDGMENTS

The research leading to these results has received funding from the People Programme (Marie Curie Actions) of the European Union’s Seventh Framework Programme (FP7/2007-2013) under REA grant agreement Nr. 291734 (T.F.) and ERC grant Nr. 250152 (N.B.). We thank Tiago Paixão, Georg Rieckh, Thomas Sokolowski and Marcin Zagorski for critical reading of the manuscript.

-
- [1] T. Yamane and J. J. Hopfield. Experimental evidence for kinetic proofreading in the aminoacylation of tRNA by synthetase. *Proceedings of the National Academy of Sciences*, 74(6):2246–2250, June 1977.
 - [2] J. J. Hopfield. Kinetic Proofreading: A New Mechanism for Reducing Errors in Biosynthetic Processes Requiring High Specificity. *Proceedings of the National Academy of Sciences*, 71(10):4135–4139, October 1974.
 - [3] Thierry Mora. Physical limit to concentration sensing amid spurious ligands. *arXiv:1504.07203 [physics, q-bio]*, April 2015. arXiv: 1504.07203.
 - [4] Peter S. Swain and Eric D. Siggia. The Role of Proofreading in Signal Transduction Specificity. *Biophysical Journal*, 82(6):2928–2933, June 2002.
 - [5] Jeffrey M. Skerker, Barrett S. Perchuk, Albert Siryaporn, Emma A. Lubin, Orr Ashenberg, Mark Goulian, and Michael T. Laub. Rewiring the Specificity of Two-Component Signal Transduction Systems. *Cell*, 133(6):1043–1054, June 2008.
 - [6] Margaret E. Johnson and Gerhard Hummer. Nonspecific binding limits the number of proteins in a cell and shapes their interaction networks. *Proceedings of the National Academy of Sciences*, 108(2):603–608, 2011.
 - [7] Jingshan Zhang, Sergei Maslov, and Eugene I. Shakhnovich. Constraints imposed by non-functional proteinprotein interactions on gene expression and proteome size. *Molecular systems biology*, 4(1), 2008.
 - [8] Thomas E. Ouldrige and Pieter Reintjes Wolde. The Robustness of Proofreading to Crowding-Induced Pseudoprocessivity in the MAPK Pathway. *Biophysical Journal*, 107(10):2425–2435, November 2014.
 - [9] Michael A. Rowland and Eric J. Deeds. Crosstalk and

- the evolution of specificity in two-component signaling. *Proceedings of the National Academy of Sciences*, 111(15):5550–5555, April 2014.
- [10] T. W. McKeithan. Kinetic proofreading in T-cell receptor signal transduction. *Proceedings of the National Academy of Sciences*, 92(11):5042–5046, May 1995.
- [11] Jean-Benoit Lalanne and Paul François. Principles of Adaptive Sorting Revealed by in silico Evolution. *Physical Review Letters*, 110(21):218102, May 2013.
- [12] Arvind Murugan, James Zou, and Michael P. Brenner. Undesired usage and the robust self-assembly of heterogeneous structures. *Nature communications*, 6, 2015.
- [13] Peter H. Von Hippel, Arnold Revzin, Carol A. Gross, and Amy C. Wang. Non-specific DNA binding of genome regulating proteins as a biological control mechanism: 1. The lac operon: equilibrium aspects. *Proceedings of the National Academy of Sciences*, 71(12):4808–4812, 1974.
- [14] Zeba Wunderlich and Leonid A. Mirny. Different gene regulation strategies revealed by analysis of binding motifs. *Trends in Genetics*, 25(10):434–440, October 2009.
- [15] Jason M. Johnson, Stephen Edwards, Daniel Shoemaker, and Eric E. Schadt. Dark matter in the genome: evidence of widespread transcription detected by microarray tiling experiments. *Trends in Genetics*, 21(2):93–102, February 2005.
- [16] Sebastian J. Maerkl and Stephen R. Quake. A Systems Approach to Measuring the Binding Energy Landscapes of Transcription Factors. *Science*, 315(5809):233–237, January 2007.
- [17] Sylvie Rockel, Marcel Geertz, Korneel Hens, Bart Deplancke, and Sebastian J. Maerkl. iSLIM: a comprehensive approach to mapping and characterizing gene regulatory networks. *Nucleic acids research*, page gks1323, 2012.
- [18] Ulrich Gerland, J. David Moroz, and Terence Hwa. Physical constraints and functional characteristics of transcription factor-DNA interaction. *Proceedings of the National Academy of Sciences*, 99(19):12015–12020, 2002.
- [19] Lacramioara Bintu, Nicolas E Buchler, Hernan G Garcia, Ulrich Gerland, Terence Hwa, Jan Kondev, and Rob Phillips. Transcriptional regulation by the numbers: models. *Current Opinion in Genetics & Development*, 15(2):116–124, April 2005.
- [20] Anne-Laure Todeschini, Adrien Georges, and Reiner A. Veitia. Transcription factors: specific DNA binding and specific gene regulation. *Trends in Genetics*, 30(6):211–219, 2014.
- [21] Adrian P. Bird. Gene number, noise reduction and biological complexity. *Trends in Genetics*, 11(3):94–100, March 1995.
- [22] Rob Phillips. Napoleon Is in Equilibrium. *Annual Review of Condensed Matter Physics*, 6(1):85–111, 2015.
- [23] G. K. Ackers, A. D. Johnson, and M. A. Shea. Quantitative model for gene regulation by lambda phage repressor. *Proceedings of the National Academy of Sciences*, 79(4):1129–1133, February 1982.
- [24] Justin B. Kinney, Anand Murugan, Curtis G. Callan, and Edward C. Cox. Using deep sequencing to characterize the biophysical mechanism of a transcriptional regulatory sequence. *Proceedings of the National Academy of Sciences*, 107(20):9158–9163, May 2010.
- [25] Sarah A. Cepeda-Humerez, Georg Rieckh, and Gašper Tkačik. Stochastic proofreading mechanism alleviates crosstalk in transcriptional regulation. *arXiv:1504.05716 [q-bio]*, April 2015. arXiv: 1504.05716.
- [26] S. Mangan and U. Alon. Structure and function of the feed-forward loop network motif. *Proceedings of the National Academy of Sciences*, 100(21):11980–11985, October 2003.
- [27] Gašper Tkačik and Aleksandra M. Walczak. Information transmission in genetic regulatory networks: a review. *Journal of Physics: Condensed Matter*, 23(15):153102, April 2011.
- [28] Julien O. Dubuis, Gašper Tkačik, Eric F. Wieschaus, Thomas Gregor, and William Bialek. Positional information, in bits. *Proceedings of the National Academy of Sciences*, 110(41):16301–16308, October 2013.
- [29] T. Friedlander and N. Brenner. Adaptive response and enlargement of dynamic range. *Mathematical Biosciences and Engineering*, 8(2):515–528, 2011.
- [30] T. Friedlander and N. Brenner. Cellular properties and population asymptotics in the population balance equation. *Physical review letters*, 101(1):18104, 2008.
- [31] George von Dassow, Eli Meir, Edwin M. Munro, and Garrett M. Odell. The segment polarity network is a robust developmental module. *Nature*, 406(6792):188–192, July 2000.
- [32] Joshua L. Payne and Andreas Wagner. The Robustness and Evolvability of Transcription Factor Binding Sites. *Science*, 343(6173):875–877, February 2014.
- [33] David L. Stern and Virginie Orgogozo. Is genetic evolution predictable? *Science*, 323(5915):746–751, 2009.
- [34] P. H. Von Hippel and O. G. Berg. On the specificity of DNA-protein interactions. *Proceedings of the National Academy of Sciences*, 83(6):1608, 1986.
- [35] Xin He, Md. Abul Hassan Samee, Charles Blatti, and Saurabh Sinha. Thermodynamics-Based Models of Transcriptional Regulation by Enhancers: The Roles of Synergistic Activation, Cooperative Binding and Short-Range Repression. *PLoS Comput Biol*, 6(9):e1000935, September 2010.
- [36] Marc S. Sherman and Barak A. Cohen. Thermodynamic State Ensemble Models of cis-Regulation. *PLoS Comput Biol*, 8(3):e1002407, March 2012.
- [37] Walid D Fakhouri, Ahmet Ay, Rupinder Sayal, Jacqueline Dresch, Evan Dayringer, and David N Arnosti. Deciphering a transcriptional regulatory code: modeling short-range repression in the Drosophila embryo. *Molecular Systems Biology*, 6(1):n/a–n/a, January 2010.
- [38] Franz M. Weinert, Robert C. Brewster, Mattias Rydenfelt, Rob Phillips, and Willem K. Kegel. Scaling of Gene Expression with Transcription-Factor Fugacity. *Physical Review Letters*, 113(25):258101, December 2014.
- [39] Otto G. Berg and Peter H. von Hippel. Selection of DNA binding sites by regulatory proteins: Statistical-mechanical theory and application to operators and promoters. *Journal of Molecular Biology*, 193(4):723–743, February 1987.
- [40] Shalev Itzkovitz, Tsvi Tlusty, and Uri Alon. Coding limits on the number of transcription factors. *BMC Genomics*, 7(1):239, September 2006.
- [41] François Spitz and Eileen E. M. Furlong. Transcription factors: from enhancer binding to developmental control. *Nature Reviews Genetics*, 13(9):613–626, September 2012.
- [42] Felipe Merino, Benjamin Bouvier, and Vlad Cojocaru. Cooperative DNA Recognition Modulated by an Interplay between Protein-Protein Interactions and DNA-

- Mediated Allostery. *PLoS Comput Biol*, 11(6):e1004287, June 2015.
- [43] Leonid A. Mirny. Nucleosome-mediated cooperativity between transcription factors. *Proceedings of the National Academy of Sciences*, 107(52):22534–22539, December 2010.
- [44] Nicolas E. Buchler, Ulrich Gerland, and Terence Hwa. On schemes of combinatorial transcription logic. *Proceedings of the National Academy of Sciences*, 100(9):5136–5141, April 2003.
- [45] Guy Shinar, Erez Dekel, Tsvi Tlusty, and Uri Alon. Rules for biological regulation based on error minimization. *Proceedings of the National Academy of Sciences of the United States of America*, 103(11):3999–4004, March 2006.
- [46] Georg Rieckh and Gašper Tkačik. Noise and Information Transmission in Promoters with Multiple Internal States. *Biophysical Journal*, 106(5):1194–1204, March 2014.
- [47] Vered Sasson, Irit Shachrai, Anat Bren, Erez Dekel, and Uri Alon. Mode of Regulation and the Insulation of Bacterial Gene Expression. *Molecular Cell*, 46(4):399–407, May 2012.
- [48] Michael B. Clark, Paulo P. Amaral, Felix J. Schlesinger, Marcel E. Dinger, Ryan J. Taft, John L. Rinn, Chris P. Ponting, Peter F. Stadler, Kevin V. Morris, Antonin Morillon, Joel S. Rozowsky, Mark B. Gerstein, Claes Wahlestedt, Yoshihide Hayashizaki, Piero Carninci, Thomas R. Gingeras, and John S. Mattick. The Reality of Pervasive Transcription. *PLoS Biol*, 9(7):e1000625, July 2011.
- [49] Alexander J. Stewart, Sridhar Hannenhalli, and Joshua B. Plotkin. Why Transcription Factor Binding Sites Are Ten Nucleotides Long. *Genetics*, 192(3):973–985, November 2012.
- [50] Murat Tuğrul, Tiago Paixão, Nicholas H. Barton, and Gašper Tkačik. Dynamics of transcription factor binding site evolution. *arXiv:1506.05162 [q-bio]*, June 2015. arXiv: 1506.05162.

III. SUPPLEMENTARY INFORMATION

A. Basic model – analytical solution

We assume that the genome of a cell contains M “target” genes, each of which is regulated by a single unique transcription factor binding site (BS). In the basic formulation, there exist also M distinct TF types, such that each TF can preferably activate its corresponding target gene by binding to its binding site. At any point in time, however, not all M TF types are present: we assume that only subsets of size $Q \leq M$ are present at some nonzero concentration, and that the optimal gene regulatory state for the cell would be to express exactly and only those genes for which the Q corresponding TFs are present.

Let regulation be determined by the (mis)match between the binding site sequence and the recognition sequence of any transcription factor. Each binding site is associated with a single TF type with which it forms a perfect match – this is the cognate TF for the given binding site. However, each site could also occasionally be bound by other (noncognate) TFs, at an energetic cost of a certain number of mismatches. Following earlier works [1, 2], we assume that the contribution of mismatches at individual positions in a binding site to the binding energy is equal, additive, and independent. We define the energy scale such that binding with cognate TF has zero energy and all other binding configurations have positive energies, proportional to the number of mismatches d , $E = \epsilon d$, where ϵ is the per-nucleotide binding energy. The unbound state has energy E_a with respect to the cognate bound state. The different states and their energies are illustrated in Fig. 3A in the main text. We employ a thermodynamic model to calculate the equilibrium binding probabilities of cognate and noncognate factors to each binding sequence.

TFs can also be non-specifically bound to the DNA. These configurations only sequester TFs from free solution, but do not directly interfere with gene expression. As explained later, we will lump together the TFs freely diffusing in the solution, as well as nonspecifically bound TFs and any other TF “reservoirs” into one effective concentration of available TFs (equivalently, we work with the chemical potential of the available TFs using the grand-canonical ensemble).

Previous studies calculated the probability of a given transcription factor to be bound or unbound to certain DNA sequences [2]. These probabilities were calculated assuming that the site is vacant or bound by the TF under study, but not bound by TFs of other types. This approach is cumbersome when a large number of TF types are considered simultaneously, because the probability that the site is bound by other factors is non-negligible, and due to steric hinderance, a site cannot be bound by more than one molecule at any given time. Previous studies also proceeded by using the canonical ensemble. These two modeling choices together make the problem of many TFs binding to multiple binding sites coupled and not easily tractable, because one would need to enumerate all possible combinations of TF-BS states. However, an alternative and much simpler approach is to employ the grand-canonical ensemble, and calculate the binding probabilities for the binding sites, rather than for the TFs. The necessary assumption is that binding sites behave independently (e.g., they are sufficiently separated on the DNA so that binding at one site does not overlap the binding at another, or if it does, this is treated explicitly). Underlying the grand-canonical ensemble is the assumption that TFs are present at sufficient copy numbers, so that the binding of a single site under consideration does not appreciably affect the chemical potential of the remaining TFs. Experimental support for such decoupling and the applicability of the grand-canonical approach has been demonstrated recently [3]. In the following we assume equal concentrations of all TF types.

We distinguish 2 contributions to crosstalk:

1. For a gene i that should be active and whose cognate TF is therefore present, error occurs if its binding site is bound by a noncognate regulator (activation out of context due to crosstalk), or if the binding site is unbound (gene is inactive). This happens with probability

$$x_1(i) = \frac{e^{-E_a} + \sum_{j \neq i} C_j e^{-\epsilon d_{ij}}}{C_i + e^{-E_a} + \sum_{j \neq i} C_j e^{-\epsilon d_{ij}}}, \quad (\text{S6})$$

where C_j is the concentration of the j th TF, d_{ij} is the number of mismatches between the j th TF consensus sequence and the binding site of gene i , ϵ the energy per mismatch and E_a the energy difference between unbound and cognate bound states; all energies are measured in units of $k_B T$.

2. For a gene i that should be inactive and whose cognate TF is therefore absent, crosstalk error only happens if its binding site is bound by a noncognate regulator (erroneous activation) rather than remaining unbound. This happens with probability

$$x_2(i) = \frac{\sum_{j \neq i} C_j e^{-\epsilon d_{ij}}}{e^{-E_a} + \sum_{j \neq i} C_j e^{-\epsilon d_{ij}}}. \quad (\text{S7})$$

See below alternative definitions for x_1 and x_2 .

Our next step is to calculate total crosstalk as a function of the above parameters (the total number of binding sites M and the number of TF types available Q). We define total crosstalk as the fraction of binding sites found in an erroneous state. To compute this fraction, we average over all possible erroneous outcomes (this is a lenient definition; other definitions can be considered, e.g. [4]). We take into account contributions from both crosstalk types: Q sites whose TFs are present (whose corresponding genes should be activated) and $M - Q$ sites whose TFs are absent (whose corresponding genes should be inactive). We assume k_1 misbinding events of the first type and k_2 of the second type and assume equivalence between the two types of error (we later relax this assumption). Another simplifying assumption is that the particular choice of Q present TFs is random (hence we average over all possible ways to choose Q out of M TF types). In reality only certain sets of TFs need to be active together in which case the genes that are co-activated could have mutually similar binding sites, especially if they were regulated by the same TF, compared to genes that are activated separately, possibly by different TFs. Later we treat a simple extension of our model where each TF can co-regulate several target genes.

To calculate the crosstalk, we average over all possible values of $k_{1,2}$ with their corresponding probabilities:

$$\begin{aligned}
X(Q, M, x_1, x_2) &= \tag{S8} \\
&= \sum_{k_1=0}^Q \sum_{k_2=0}^{M-Q} \frac{k_1 + k_2}{M} \binom{Q}{k_1} \binom{M-Q}{k_2} x_1^{k_1} (1-x_1)^{Q-k_1} x_2^{k_2} (1-x_2)^{M-Q-k_2} \\
&= \sum_{k_1=0}^Q \frac{k_1}{M} \binom{Q}{k_1} x_1^{k_1} (1-x_1)^{Q-k_1} \sum_{k_2=0}^{M-Q} \binom{M-Q}{k_2} x_2^{k_2} (1-x_2)^{M-Q-k_2} \\
&\quad + \sum_{k_1=0}^Q \binom{Q}{k_1} x_1^{k_1} (1-x_1)^{Q-k_1} \sum_{k_2=0}^{M-Q} \frac{k_2}{M} \binom{M-Q}{k_2} x_2^{k_2} (1-x_2)^{M-Q-k_2} \\
&= \frac{Qx_1}{M} \sum_{k_1=0}^Q \binom{Q-1}{k_1-1} x_1^{k_1-1} (1-x_1)^{Q-k_1} + \frac{M-Q}{M} x_2 \sum_{k_2=0}^{M-Q} \binom{M-Q-1}{k_2-1} x_2^{k_2-1} (1-x_2)^{M-Q-k_2} \\
&= \frac{Qx_1}{M} \sum_{l=-1}^{Q-1} \binom{Q-1}{l} x_1^l (1-x_1)^{Q-1-l} + \frac{M-Q}{M} x_2 \sum_{j=-1}^{M-Q-1} \binom{M-Q-1}{j} x_2^j (1-x_2)^{M-Q-1-j} \\
&= x_1 \frac{Q}{M} + x_2 \frac{M-Q}{M}.
\end{aligned}$$

Utilizing the definition of S introduced in the main text

$$\sum_j C_j e^{-\epsilon d_{ij}} = \frac{C}{Q} (Q-1) \sum_d P(d) e^{-\epsilon d} \approx C \sum_d P(d) e^{-\epsilon d} \equiv CS(\epsilon, L), \tag{S9}$$

where we approximated $Q-1 \approx Q$ which is valid for $Q \gg 1$ (an assumption we make here and throughout the paper). $S(\epsilon, L)$ is an average similarity measure between all pairs of binding sites. If binding site sequences are drawn randomly from a uniform distribution, $S = (\frac{1}{4} + \frac{3}{4} e^{-\epsilon})^L$. This is easy to derive: since individual base pairs are assumed to be statistically independent, at each position the probability of a random sequence to be identical to a given TF consensus sequence is $1/4$, whereas with probability $3/4$ it is different, implying an increase of ϵ in binding energy. Since the complete binding site consists of L independent base pairs, this expression for a single base pair is raised to the power of L .

The expressions for $x_{1,2}$ read:

$$x_1 = \frac{e^{-E_a} + CS}{\frac{C}{Q} + e^{-E_a} + CS} \tag{S10a}$$

$$x_2 = \frac{CS}{e^{-E_a} + CS}. \tag{S10b}$$

The two extreme cases occur when TF concentrations are either zero or very large. If $C = 0$, $x_1 = 1$ and $x_2 = 0$, i.e., x_1 is maximal due to binding sites that should be bound, while zero error for x_2 occurs due to binding sites that should be unbound. The total error then amounts to the fraction of genes that need to be activated $X(C = 0) = Q/M$.

At the other extreme, if $C \rightarrow \infty$, $x_1 = SQ/(1 + SQ)$ and $x_2 \approx 1$, i.e., no site is left unbound. The magnitude of x_1 error due to noncognate binding is determined by the binding site similarity S . If $QS \ll 1$, $x_1 \approx QS - (QS)^2$. The total crosstalk then amounts to $X(C \rightarrow \infty) = 1 - \frac{Q/M}{1+SQ}$. If $SQ \ll 1$, $X \approx 1 - \frac{Q}{M}(1 - SQ)$.

	x_1	x_2	crosstalk, X
	$\frac{e^{-E_a+CS}}{\frac{Q}{M} + e^{-E_a+CS}}$	$\frac{CS}{e^{-E_a+CS}}$	$\frac{Q}{M}x_1 + \frac{M-Q}{M}x_2$
$C = 0$	1	0	Q/M
$C = \infty$	$\frac{SQ}{1+SQ}$	1	$1 - \frac{Q/M}{1+SQ}$
optimal C ; only activators	$\frac{1+QZ}{1+Z/S+QZ}$	$\frac{QZ}{1+QZ}$	$\frac{Q}{M} \frac{1+QZ}{1+Z/S+QZ} + \frac{M-Q}{M} \frac{QZ}{1+QZ}$
optimal C ; activators and global repressor	$\frac{1+QZ}{1+Z/S+QZ}$	$\frac{QZ}{1+QZ}$	$\frac{Q}{M} \frac{1+QZ}{1+Z/S+QZ} + \frac{M-Q}{M} \frac{QZ}{1+QZ}$

TABLE I. Crosstalk errors in the basic model. Per-gene errors of the two types: x_1 is the error of a site whose cognate TF exists and the site should therefore be bound, but is either unbound or bound by a noncognate factor. x_2 is the error of a site whose cognate factor does not exist, and the site should therefore be unbound, but is bound by a noncognate factor. The last column shows the total crosstalk, averaged over all M sites.

Next, we analyze the dependence of crosstalk on various parameters. One unknown in these expressions is the TF concentration C . Because we are searching for a lower bound on crosstalk, we can find the concentration that minimizes X . Taking the derivative of X and solving for its zeros,

$$\frac{\partial}{\partial C} X(Q, M, x_1, x_2) = 0,$$

we find two potential extrema

$$C_{1,2}^* = \frac{Qe^{-E_a} \left(S(SMQ - Q(SQ + 2)) + M \pm \sqrt{S(M - Q)} \right)}{S(-M(SQ + 1)^2 + SQ^2(SQ + 3) + Q)},$$

but only one of them can yield non-negative concentration values (and is consistently a minimum):

$$C^* = \frac{Qe^{-E_a} \left(S(SMQ - Q(SQ + 2)) + M - \sqrt{S(M - Q)} \right)}{S(-M(SQ + 1)^2 + SQ^2(SQ + 3) + Q)}. \quad (\text{S11})$$

For small S the leading terms in the optimal concentration are

$$C^* = \frac{e^{-E_a} Q}{\sqrt{S(M - Q)}} - \frac{e^{-E_a} Q(M - 2Q)}{M - Q} - \frac{e^{-E_a} Q^2(2M - 3Q)\sqrt{S}^{3/2}}{M - Q} + O[S]. \quad (\text{S12})$$

Substituting Eq. (S11) back into Eq. (S8) yields the minimal achievable crosstalk:

$$X^* = \frac{Q}{M} \left(-S(M - Q) + 2\sqrt{S(M - Q)} \right). \quad (\text{S13})$$

Substituting C^* into the single gene crosstalk expressions Eqs. (S6)-(S7), we obtain the minimal per-gene crosstalk

$$x_1^* = \sqrt{S(M - Q)} \quad (\text{S14a})$$

$$x_2^* = SQ \left(\frac{1}{\sqrt{S(M - Q)}} - 1 \right). \quad (\text{S14b})$$

Since crosstalk must be in the range $[0,1]$ and $M \geq Q$, this solution is only valid under the condition that $S(M - Q) < 1$. Thus, minimal crosstalk has 3 regimes:

1. For $S > 1/(M - Q)$ crosstalk is minimized by taking $C = 0$. This is the “no regulation” regime. In this case, crosstalk amounts to Q/M , which is simply the fraction of genes that were supposed to be activated (but are not due to lack of their TFs).
2. For $Q > Q_{\max}(S, M)$ crosstalk is minimized by taking $C \rightarrow \infty$; this is the “constitutive regime.” $Q_{\max}(S, M)$ is given by two of the roots of the 4th order equation, $S(M + SMQ - 2Q - SQ^2) - \sqrt{S(M - Q)} = 0$, solved for Q . We find the boundaries between the 3 different regulatory regimes by solving for $C^*(S, M, Q) = 0$.
3. Otherwise, there is an optimal concentration $0 < C^* < \infty$, given by Eq. (S11), that minimizes crosstalk; this is the “regulation regime.”

The boundary between the first and third region is at $S^* = \frac{1}{M - Q}$ and the boundary between the second and the third is at $S^* = \frac{-2M + 3Q \pm \sqrt{Q(5Q - 4M)}}{2Q(M - Q)}$. Hence, the second region (where $C^* = \infty$) only applies for $Q > \frac{4M}{5}$. Fig S1 illustrates the dependence of the TF concentration C^* , which minimizes crosstalk, on the number of co-activated genes Q . It demonstrates how the range in which $0 < C^* < \infty$ gets narrower when S increases. Fig S2 demonstrates crosstalk and C^* values for $M = 20 \cdot 10^3$ (compare to Fig. 3 in the main text with $M = 5 \cdot 10^3$).

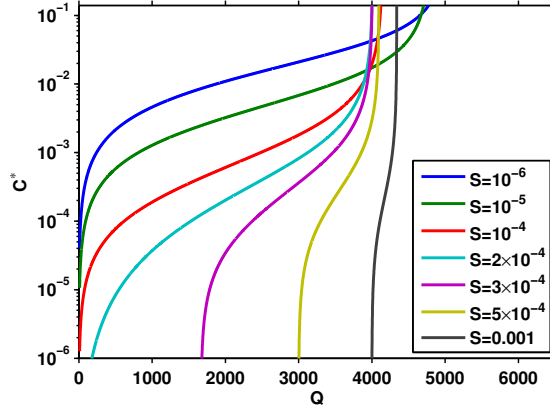


FIG. S1. **At fixed M , the optimal TF concentration, C^* , diverges with the number of co-activated genes, Q .** This leads to the “constitutive regime,” where crosstalk is mathematically minimized by taking $C = \infty$. Shown is the optimal concentration C^* as a function of the number of co-activated genes Q , for various S values; M is fixed at $5 \cdot 10^3$. The value of Q at which C diverges depends on S . For small Q , we require $M - 1/S < Q$, otherwise the optimal concentration is in the $C^* = 0$ regime. For the lower S values crosstalk can be minimized for $0 < Q < Q_{\max} < M$, whereas for higher S values there exists also a value for Q_{\min} , such that $0 < Q_{\min} < Q < Q_{\max} < M$. In other words, higher S leads to a narrower range of Q where the crosstalk can be effectively minimized.

B. Basic model with regulation by repressors only

Our basic model assumed that all gene regulation is achieved by using specific activators to drive the expression of genes that would otherwise remain inactive. An alternative formulation of the problem postulates that genes are strongly expressed without TFs bound to their regulatory sites, but need to be repressed by the binding of specific regulators to stop their expression. Indeed, many bacterial genes seem to be regulated in this way. We thus studied this complementary model, in which all regulators are repressors instead of activators. We assume, as before, that Q out of M genes should be active, but now this implies that $M - Q$ types of cognate repressors are present for all the genes that should remain inactive.

The expressions for crosstalk per gene that should be active (x_1) or inactive (x_2) read:

$$x_1 = \frac{CS}{e^{-E_a} + CS} \quad (\text{S15a})$$

$$x_2 = \frac{e^{-E_a} + CS}{\frac{C}{M - Q} + e^{-E_a} + CS}. \quad (\text{S15b})$$

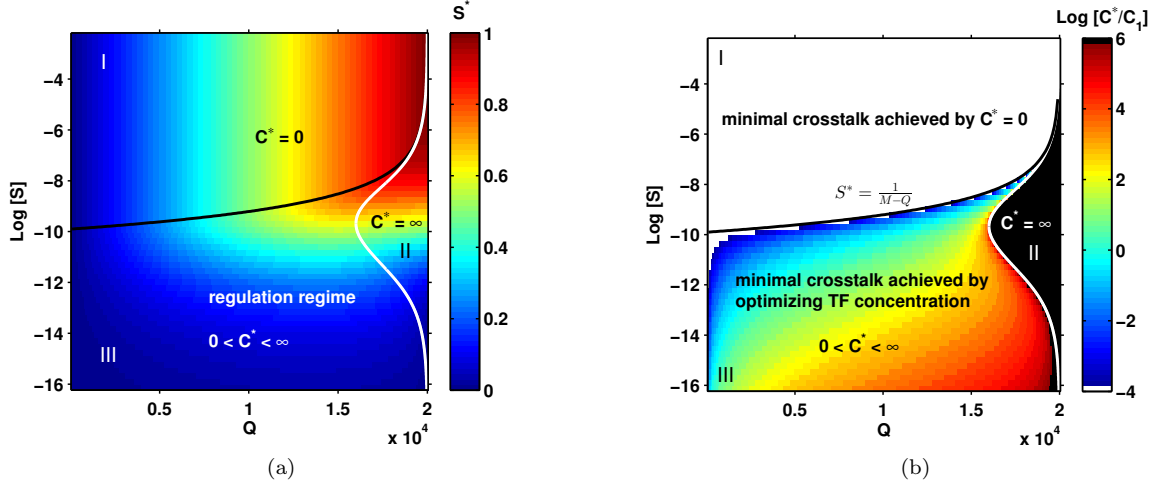


FIG. S2. **Crosstalk in the basic model for $M = 20 \cdot 10^3$.** Panel (a) shows the minimal crosstalk, X^* ; panel (b) shows the optimal TF concentration, C^* . These results are analogous to Fig. 3 of the main paper, which is computed for $M = 5 \cdot 10^3$. The results for two different M are qualitatively similar and show 3 different regimes of regulation. We make the following observations: (i) for larger M , the $C^* = 0$ regime expands to include lower S values, as expected from the analytical solution for the regime boundaries; (ii) if the fraction of co-activated genes, Q/M , remains constant, the crosstalk *increases* with M , as it also depends on the absolute number of inactive genes $M - Q$ (see Eq. (S13)). The discrepancies at small Q between the black solid curve separating the “no regulation” and “regulation” regimes, and the numerically computed C^* values are due to the approximation $Q - 1 \approx Q$.

The total crosstalk is still

$$X = \frac{Q}{M}x_1 + \frac{M - Q}{M}x_2. \quad (\text{S16})$$

Eqs. (S15) are the mathematically identical to Eqs. (S10), where the roles of Q and $M - Q$ are simply swapped. Not surprisingly, the minimal crosstalk in this case is:

$$x_1^* = \sqrt{QS} \quad (\text{S17a})$$

$$x_2^* = \frac{(M - Q)S(QS - 1)}{QS + \sqrt{QS}} \quad (\text{S17b})$$

$$X^* = \frac{M - Q}{M}(2\sqrt{QS} - QS), \quad (\text{S17c})$$

which is valid for $S < 1/Q$.

The optimal TF concentration that minimizes crosstalk is now

$$C^* = \frac{e^{-E_a}(M - Q)(1 - QS)}{\sqrt{QS} + QS(2 - QS) + MS(QS - 1)}. \quad (\text{S18})$$

The minimal crosstalk and optimal concentration are illustrated in Fig S3. It retains the 3 regulatory regimes observed with activators only:

1. For $S > 1/Q$ we obtain the “no regulation” regime where crosstalk is minimized by taking $C = 0$.
2. For $Q < Q_{\min}(S, M)$ we obtain the “constitutive regime” where crosstalk is minimized by taking $C \rightarrow \infty$. Q_{\min} is obtained when C^* of Eq. (S18) diverges (the denominator equals to zero).
3. Otherwise, there is an optimal concentration $0 < C^* < \infty$, given by Eq. (S18), that minimizes crosstalk; this is the “regulation regime.”

The three regions are marked with Roman numerals, in accordance with Fig. 3 of the main text. The boundaries between the three regimes are now: $S^* = 1/Q$ (between regimes I and III) and $S^* = \frac{M-3Q \pm \sqrt{(M-Q)(M-5Q)}}{2Q(M-Q)}$ (between regime II to both I and III).

The results are clearly a mirror image of the results shown in Fig. 3 of the main text for the activator-only basic model. They can be obtained simply by mapping $Q \rightarrow M - Q$. Since we keep the convention that Q is the number of genes that are active, the difference in regulation strategies amounts to having either Q activator types and keeping $M - Q$ binding sites unbound (activator-only) or having $M - Q$ repressor types and keeping Q binding sites unbound. Comparing the expressions for minimal crosstalk Eq. (S17c) to Eq. (S13) we conclude that crosstalk depends on the *fraction* of TFs that are expressed and on the *absolute number* of binding sites that need to remain unbound.

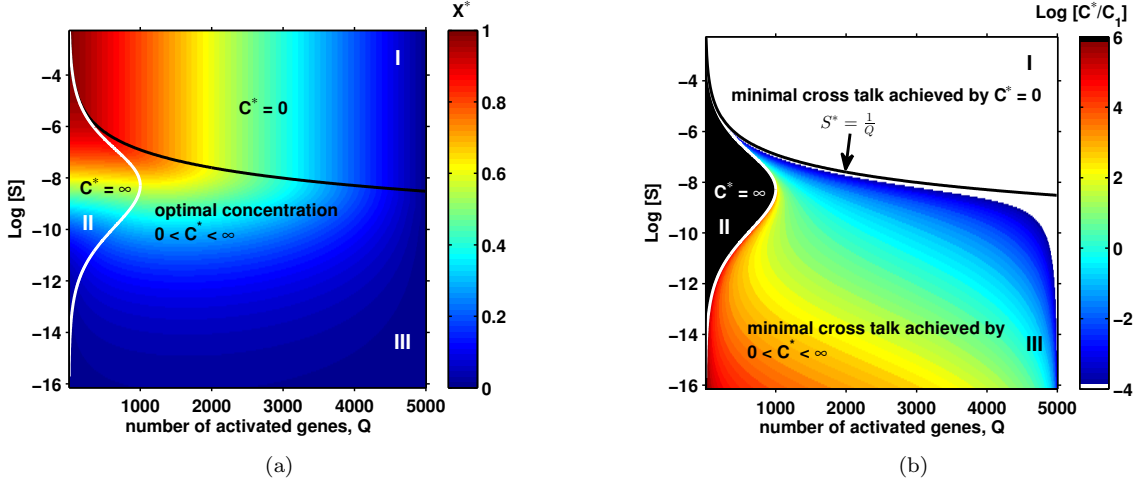


FIG. S3. **Crosstalk in the basic model with regulation by repressors alone is a mirror image of regulation with activators only.** Panel (a) shows the minimal crosstalk, X^* ; panel (b) shows the optimal TF concentration, C^* . These results are analogous to Fig. 3 of the main paper, which is computed for regulation with activators only. The observed picture is an exact mirror image of Fig. 3 of the main text, namely Q maps to $M - Q$, where we keep the convention that Q denotes the number of genes that should be active. The difference is that in the activator-model activating Q genes requires Q types of activators, whereas in the repressor model this requires $M - Q$ types of repressors.

C. Breaking the symmetry between the two crosstalk types

In our basic model we made a simplifying assumption that the two crosstalk types, x_1 and x_2 , have equal weights: not activating a gene that should be active or erroneously activating a gene that should be inactive are assumed to be equally disadvantageous. We now relax this symmetry by allowing different weights, a and b , for the two crosstalk types, to model possible differences in their biological significance. Eq. (S8) for the total crosstalk now takes the form:

$$X = a \frac{Q}{M} x_1 + b \frac{M - Q}{M} x_2. \quad (\text{S19})$$

The expression for the optimal TF concentration then reads:

$$C^*(a, b) = \frac{e^{-E_a} Q (\pm \sqrt{abS(M-Q)} - S(aQ - b(M-Q)(1 + SQ)))}{S(aSQ^2 - b(M-Q)(1 + SQ)^2)}, \quad (\text{S20})$$

where again only one of the two solutions yields non-negative concentration values. The resulting minimal crosstalk is:

$$X^*(a, b) = \frac{Q}{M} (-Sb(M-Q) + 2\sqrt{abS(M-Q)}). \quad (\text{S21})$$

Setting $a = b = 1$ reduces the above formula to the previous solution, Eqs. (S11)-(S13). Note the asymmetry between the two crosstalk types: if $b = 0$, i.e., when crosstalk in genes that should remain inactive is insignificant, the

minimal achievable crosstalk equals zero. This is not true in the other extreme case, when $a = 0$. In the main text we show that the three different regulatory regimes still exist under this generalized definition of crosstalk, but their boundaries may shift.

D. Breaking the symmetry between the co-activated genes

In our basic model we imposed full symmetry between the Q co-activated genes: they contributed equally to crosstalk and all Q types of TFs were assumed to exist in equal concentrations. We now relax these assumptions. We examine the situation in which a fraction h of these Q genes is more important to the functioning of the cell. Mathematically, we postulate that the per-gene crosstalk error for the important genes contributes with a γ -times higher weight to the total crosstalk relative to the non-important genes. We introduce an additional degree of freedom to the model, by allowing the concentration of the TFs to split unevenly between important and other genes: each important gene has TFs present at concentration C_0 , while a TF of a non-important gene is present at concentration $C_1 = \eta C_0$.

As $hQC_0 + (1-h)QC_1 = C$ we obtain:

$$C_1 = \frac{C}{Q} \frac{1}{(1-h+h\eta)} \quad (\text{S22a})$$

$$C_0 = \eta C_1 = \frac{C}{Q} \frac{\eta}{(1-h+h\eta)} \quad (\text{S22b})$$

If either $h = 0$ or $\eta = 1$ this reduces back to the basic model with $C_0 = C_1 = C/Q$. The total crosstalk now takes the form:

$$X = \gamma h \frac{Q}{M} x_0 + (1-h) \frac{Q}{M} x_1 + \frac{M-Q}{M} x_2 \quad (\text{S23a})$$

$$x_0 = \frac{e^{-E_a} + CS \left(1 - \frac{\eta}{Q(1+h(\eta-1))}\right)}{e^{-E_a} + \frac{\eta C/Q}{1+h(\eta-1)} + CS \left(1 - \frac{\eta}{Q(1+h(\eta-1))}\right)} \quad (\text{S23b})$$

$$x_1 = \frac{e^{-E_a} + CS \left(1 - \frac{1}{Q(1+h(\eta-1))}\right)}{e^{-E_a} + \frac{C/Q}{1+h(\eta-1)} + CS \left(1 - \frac{1}{Q(1+h(\eta-1))}\right)} \quad (\text{S23c})$$

$$x_2 = \frac{CS}{e^{-E_a} + CS}, \quad (\text{S23d})$$

where x_0 is the per-gene error of the important genes, x_1 is the error of the non-important genes that need to be activated, and x_2 , as before, denotes crosstalk of the genes that need to be kept inactive.

We can optimize numerically for both the total TF concentration C and the factor η by which the TF concentration of the important genes is amplified. Alternatively, we can assume that C remains fixed at the optimal value for the case where all genes are equally important ($\gamma = 1$ or $h = 0$), and only optimize for η . We displayed the latter option in Fig. 4B in the main text, to explore crosstalk at varying h under equal resource constraints.

The special case when only a single gene is important is analytically solvable assuming $Q \gg 1$, yielding:

$$X_{1 \text{ important gene}}^* \approx \frac{-SQ(M-Q) + 2\sqrt{S(M-Q)}(Q-1 + \sqrt{\gamma})}{M}. \quad (\text{S24})$$

In particular the per-gene errors read:

$$x_0^* = \frac{\sqrt{S(M-Q)}}{\sqrt{\gamma}} \quad (\text{S25a})$$

$$x_1^* = \sqrt{S(M-Q)} \quad (\text{S25b})$$

$$x_2^* = \frac{-SQ(M-Q) + \sqrt{S(M-Q)}(Q-1 + \sqrt{\gamma})}{M-Q}. \quad (\text{S25c})$$

The error of the single important gene can be reduced at most by a factor of $\sqrt{\gamma}$ relative to the other co-activated genes. The x_1^* error for the other $Q-1$ genes remains the same, because we assumed that $Q \gg 1$. Interestingly, the $M-Q$ genes that need to be kept inactive suffer an increase in crosstalk as a consequence of protecting the important gene.

E. Every transcription factor regulates Θ genes

In the basic model we considered a regulatory scheme in which every gene has its own unique TF type. This allows for maximal flexibility in regulating each gene individually. Real gene regulatory networks typically have fewer TFs than the number of target genes, so that at least some transcription factors regulate several genes. Here we consider a simple extension of the basic model, in which each TF regulates Θ genes rather than one. We assume no overlap between the sets of genes regulated by various TFs, so that the total number of TFs species is now Θ times smaller than before. If Q genes should be active, then Q/Θ TF species should be present in a given condition. Assuming that $Q/\Theta \gg 1$, we can approximate $Q/\Theta - 1 \approx Q/\Theta$ as before. The only change from the basic crosstalk formulation is in x_1 , because the concentration of cognate factors is now Θ times larger than before:

$$x_1^\Theta = \frac{e^{-E_a} + CS}{\frac{C}{Q/\Theta} + e^{-E_a} + CS} \quad (\text{S26a})$$

$$x_2^\Theta = \frac{CS}{e^{-E_a} + CS}. \quad (\text{S26b})$$

This formulation is analytically solvable, yielding

$$X_\Theta^* = \frac{Q}{\Theta M} \left(-S(M - Q) + 2\sqrt{S\Theta(M - Q)} \right) \quad (\text{S27a})$$

$$x_1^{\Theta*} = \frac{\sqrt{S(M - Q)}}{\sqrt{\Theta}} \quad (\text{S27b})$$

$$x_2^{\Theta*} = \frac{SQ}{\Theta} \left(\frac{\Theta}{\sqrt{S(M - Q)}} - 1 \right) \quad (\text{S27c})$$

$$C_\Theta^* = \frac{e^{-E_a} Q (\Theta - S(M - Q))}{S^2(M - Q)Q + S(M - 2Q)\Theta + \sqrt{S(M - Q)}\Theta^{3/2}}. \quad (\text{S27d})$$

For small S the leading term in the optimal concentration is

$$C_\Theta^* = \frac{1}{\sqrt{\Theta}} \frac{e^{-E_a} Q}{\sqrt{S(M - Q)}} + O(1). \quad (\text{S28})$$

Compared to the basic model result of Eq. (S12), the optimal TF concentration is now reduced by a factor of $\sqrt{\Theta}$, as is the minimal crosstalk error of the first type, $x_1^{\Theta*}$. The dependence on Θ of the crosstalk of the second type, $x_2^{\Theta*}$, is more complicated. These gains in crosstalk have, however, been achieved by sacrificing the ability to regulate each gene individually: now, the smallest set of genes that can be co-activated is of size Θ . Typically, TFs might constitute $\gtrsim 10\%$ of the genes [5]; with $\Theta \sim 10$, the crosstalk could be reduced by a factor of ~ 3 at best.

F. Alternative crosstalk definition

In the basic setup presented in the main text, we considered “activation out-of-context”—i.e., activation by the binding of a noncognate TF when the cognate TF is present (but not bound)—to be a crosstalk state. Our reasoning was motivated by viewing transcriptional regulation as a signal transmission apparatus. In this interpretation, gene activation by a noncognate TF amounts to generating a response (transcriptional activity) to a wrong input signal. Consequently, this should count as crosstalk, despite the fact that (by chance) the correct signal was simultaneously present in the cell. This is perhaps easiest to appreciate if one considers more realistic setups in which genes are not simply “ON” and “OFF”, but can be quantitatively regulated by the level of their cognate TF. In such a model, there might be two TFs present and varying in concentration as a function of time: one cognate for the gene of interest and one not. In this case it is clear that the correct response of the gene is to track the changes in the cognate TF, and not to simply be expressed in a constant “ON” state; consequently, tracking the noncognate TF due to crosstalk is obviously an error, even if the cognate TF is present at the same time.

One could, however, argue that “activation-out-of-context” shouldn’t be considered as an error state. If the presence or absence of TF signals really is a binary variable and if the binary response is defined solely by the state of transcriptional activity (activation/inactivation of gene), then when the presence of the signal matches the response state, the regulation outcome is correct, irrespective of the detailed molecular state at the promoter. For example, for

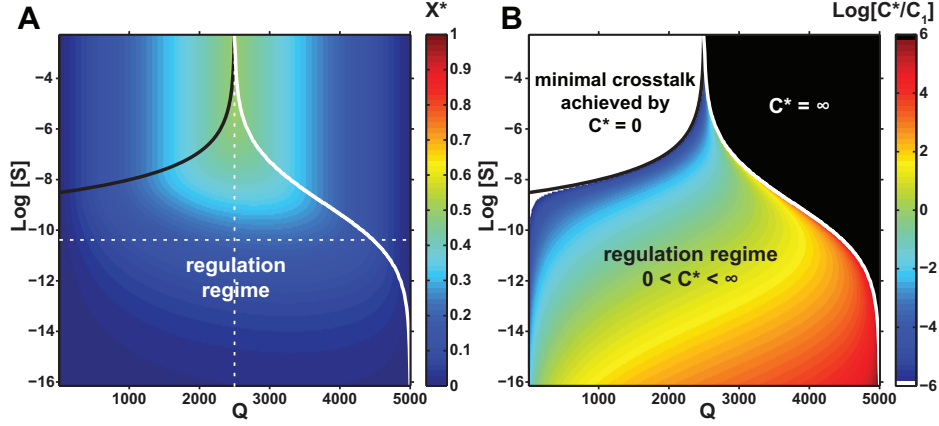


FIG. S4. **Basic model with alternative crosstalk definition also exhibits three distinct regulation regimes.** The alternative definition does not count “activation out-of-context” as an error state. (A) Minimal crosstalk error, X^* , shown in color, as a function of the number of coactivated genes Q , and binding site similarity S . (B) Optimal TF concentration C^* , that minimizes the crosstalk, relative to C_0 , the optimal concentration at the baseline parameters (see main text).

a gene whose cognate TF is present, activation by any means (either by cognate or noncognate binding) is the correct response. In this scenario, the “out-of-context activation” is actually what one might call beneficial crosstalk: here, noncognate TF can be seen as helping to activate the gene when the cognate TF is also present. For a gene whose cognate TF is absent, activation is still an incorrect response, like before.

Hence, $x_2(i)$ retains the same expression, but $x_1(i)$ changes to

$$x_1(i) = \frac{e^{-E_a}}{C_i + e^{-E_a} + \sum_{j \neq i} C_j e^{-\epsilon d_{ij}}}.$$

As shown in Fig. S4, optimizing C results in three distinct regulatory regimes, like in the default basic setup. For small S in the regulation regime, the optimal C is given to the leading order by:

$$C^* \sim \frac{e^{-E_a}}{\sqrt{S}} \frac{Q}{\sqrt{M-Q}}$$

The minimal crosstalk error at the optimal concentration C^* is given by

$$X^* = -SQ + 2 \frac{Q}{M} \sqrt{S(M-Q)(1+SQ)}$$

G. Estimating the binding site similarity, S

1. Optimal packing

In real organisms, binding site sequences for different genes could depart from a random distribution (even after taking into account the statistical structure of the genomic background). For example, to achieve high specificity of regulation, we could hypothesize that binding site sequences evolved to minimize the overlap between any pair of consensus sequences. To explore the crosstalk limit under such optimal use of sequence space and contrast it with the random choice of binding sites in our basic model, we synthetically constructed binding site sequences that are as distinct as possible. Specifically, our optimal codes are described by a parameter d_{\min} , which is the minimum required number of basepair differences between any pair of binding site sequences. The problem of choosing M sequences of length L such that each pair differs by at least d_{\min} is not tractably solvable in general. We construct numerical approximations to these optimal codes using the following algorithm:

1. Generate all possible sequences of length L and store them in a list called *words*. Create an empty list, called *codewords*, which will store the binding site sequences.

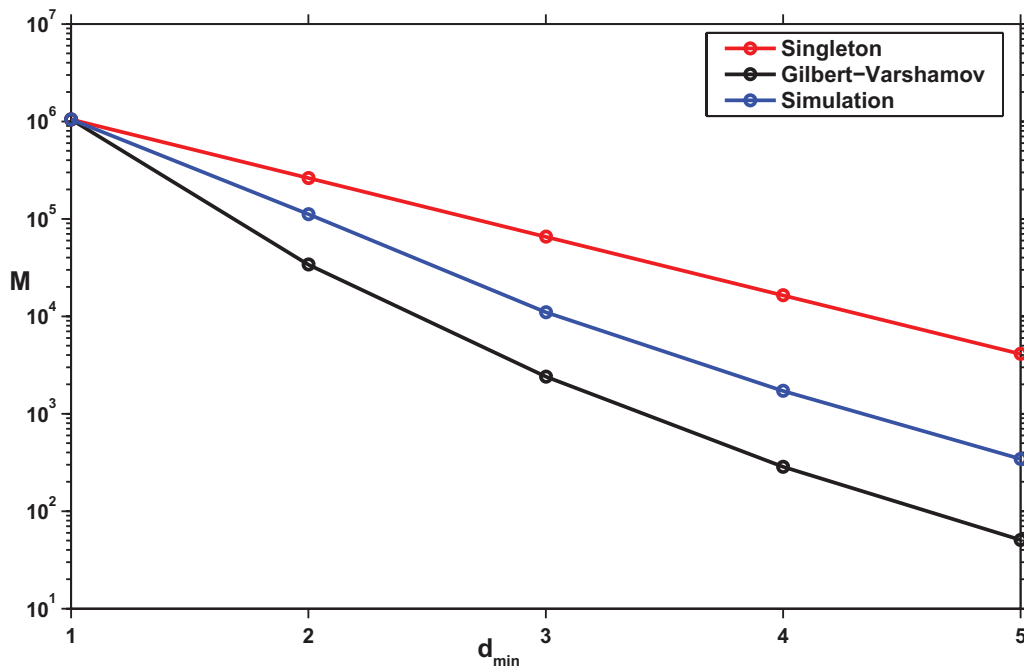


FIG. S5. **Bounds on the maximal number of binding site sequences for different d_{\min} with binding sites of length $L = 10$.** Two bounds from the coding theory (Singleton upper bound and Gilbert-Varshamov lower bound) are shown together with the values of M obtained by our numerical approximation procedure. For $d_{\min} = 1$ there are $M = 4^{10} \approx 10^6$ possible sequences where all sequence pairs are at least d_{\min} distant from each other, but the number quickly decreases with increasing d_{\min} .

2. Pick the first entry, s , from the list *words*, to be a binding site sequence, and append it to the list *codewords*.
3. Erase s and all of its Hamming neighbours at distance strictly less than d_{\min} from the list *words*.
4. If the list *words* is not empty, repeat from step 2. If the list *words* is empty, stop.

When the procedure terminates, the list *codewords* will contain binding site sequences that are separated by at least d_{\min} mismatches. The outcome of this procedure depends on the initial ordering of the list of all possible sequences. The procedure is not guaranteed to generate the maximal set of sequences satisfying the Hamming distance criteria. From the list of generated binding site sequences, we obtain $P(d)$, the distribution of mismatch distances between all pairs of binding sites, and hence obtain the value of S as

$$\tilde{S}(d_{\min}) = \sum_{d \geq d_{\min}} P(d) e^{-\epsilon d}$$

$d_{\min} = 0$ corresponds to the "random code" and results in $\tilde{S}(d_{\min} = 0) = S = (\frac{1}{4} + \frac{3}{4}e^{-\epsilon})^L$. Note that increasing d_{\min} decreases the maximum possible M as sequences move further apart in sequence space whose volume is fixed by L . A well-known upper bound on the number of sequences satisfying the Hamming distance criterion is the Singleton bound: $M(d_{\min}, L) \leq 4^{L-d_{\min}+1}$. As shown in Fig. S5, with $L = 10$ and $d_{\min} = 4$, we already have $M \leq 16384$. As L becomes smaller, the possible range of M also decreases. This suggests that prokaryotes are capable of having optimally packed binding site sequences, because they typically have $L > 10$ and $M < 10^4$. On the other hand, eukaryotes have smaller L and larger M and might not have enough sequence space to pack it optimally.

2. Saturating model of TF-DNA binding energy

It has been experimentally observed that the binding energy between TF and DNA saturates to a constant value after a certain number of mismatches between the TF's cognate sequence and the DNA sequence in question [6]. We consider such a saturating energy model, characterized by a parameter d_0 , the number of mismatches after which binding energy saturates. The binding energy is given by $E(d) = \epsilon \min(d, d_0)$. We obtain S as

$$\tilde{S}(d_0) = \sum_d P(d)e^{-E(d)}$$

where $P(d)$ is the distribution of mismatch distances between all pairs of binding sites picked at random from the sequence space. $d_0 = L$ corresponds to a mismatch model with non-saturating energy. Decreasing d_0 limits the specificity of the TF towards binding site sequences far away from the consensus and thereby increases $\tilde{S}(d_0)$.

3. Empirical values

We obtain organism-specific estimates of S from genomic databases of the binding site sequences of different TFs [7–9]. In the main text we defined S for a genome-specific collection of TFs with the same mismatch penalty ϵ and binding sites of a specific constant length L . In real organisms, different TFs have different ϵ and L , making it difficult to directly calculate S for the whole genome. Instead we obtain a value of S for each TF by defining it as the value of S in a hypothetical genome in which all TFs have the same binding site properties (ϵ, L) as our TF. Hence, for each organism, we obtain a set of S values.

Many databases summarize the binding site sequences of TFs in Position Count Matrices (PCMs). The PCM of a TF with a binding site of length L is a $4 \times L$ matrix B with b_{ij} denoting the number of known TF binding site sequences that have nucleotide i in position j . One can obtain estimates of ϵ and L from B , and use them to calculate S . There are two broad ways to estimate ϵ and L (and hence, S) of a TF: **(a)** the information method, and **(b)**, the pseudo-count method. In (a), we calculate the information contained in the whole binding site motif and obtain an ϵ that distributes this information uniformly among all sites in an equivalent “effective” motif that has the same length as the original, but only has 0 or ϵ mismatch energy values. In (b), we obtain a “binding energy matrix” from the PCM (i.e., infer a separate binding energy at every position for every nucleotide, under the standard set of assumptions [12]) and calculate an effective mismatch energy ϵ by averaging across the energy matrix. To handle zeros in the PCM which lead to undefined energy matrix entries, (b) adds pseudo-counts to PCM entries, which is one of standard ways of dealing with the inference problem. Method (a) can, in contrast, avoid the use of pseudo-counts and, additionally, reproduces by construction the information content of each known motif, which is the key statistical property of TF specificity [10, 11]. Hence, we used (a) to infer S values in the main paper; here we report on both methods. In both the methods, we used PCMs that have that have been constructed from at least 10 distinct binding site sequences.

Information method. In this method, we first extract the length L of the binding site and compute the total information I , contained in the binding site sequences of the chosen TF:

$$I = \sum_j I_j = \sum_j \sum_i p_{ij} \log_2 \frac{p_{ij}}{q_{ij}}$$

where I_j is the information contained in position j , p_{ij} is the frequency of nucleotide i in position j , obtained in a straightforward way from B , and q_{ij} is the expected background frequency. To get rid of non-specific positions, we neglect all positions that contain information less than a certain threshold ($I_j > 0.2$ bits for position j to be considered part of the binding site). For a random genome, $q_{ij} = 0.25$ for all i and j , resulting in

$$I = 2L + \sum_{i,j} p_{ij} \log_2 p_{ij}$$

The maximum information in the motif is $2L$ bits (when $\epsilon \rightarrow \infty$) with each position contributing a maximum of 2 bits; finite ϵ this is reduced by an entropy term. Obtaining information per position $I_{pos} = I/L$, we infer an ϵ that uniformly distributes the information in the motif among individual positions. At a specific position j^* , without loss of generality, assume that $i = 4$ has the best binding energy ($= 0$). The probability of observing $i = 4$ at j^* is given by $p_4 = 1/Z$ while the probability of observing any of the three other possible nucleotides is given by $p_{1,2,3} = e^{-\epsilon}/Z$, with $Z = 1 + 3e^{-\epsilon}$ [12]. Hence,

$$\begin{aligned} I_{pos} &= 2 + \sum_i p_i \log_2 p_i \\ &= 2 - \frac{1}{Z} \log_2 Z - 3 \frac{1}{Z \ln 2} \epsilon e^{-\epsilon} - 3 \frac{e^{-\epsilon}}{Z} \log_2 Z \\ &= 2 - \log_2 Z - 3 \frac{1}{Z \ln 2} \epsilon e^{-\epsilon} \end{aligned}$$

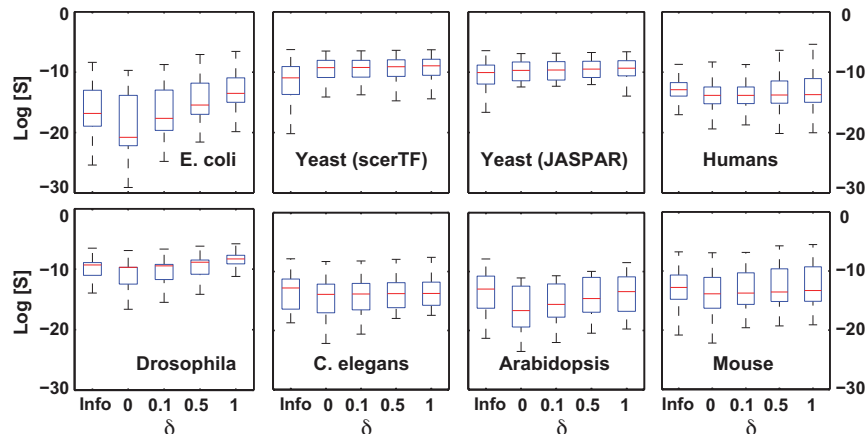


FIG. S6. **Boxplots of S for TFs from different databases.** In each panel, organism-specific (from a single database) boxplots of S are shown. The first boxplot in each panel corresponds to S values obtained from information estimates, and the remaining four correspond to S values obtained using the pseudo-count method with $\delta = 0, 0.1, 0.5, 1$ from left to right. *E. coli* TFs were obtained from RegulonDB [7] and yeast (*S. cerevisiae*) from two different databases – scerTF [9] and JASPAR [8]. All the other organism specific TFs were obtained from JASPAR. Notice that in the pseudo-count method, δ has the biggest influence on the estimates in *E. coli*. Importantly, for all other organisms, the estimates are invariant to δ and in general seem to agree with the information estimate.

The mismatch energy ϵ can be obtained from the above expression, and from ϵ and L , we obtain $S(\epsilon, L) = (\frac{1}{4} + \frac{3}{4}e^{-\epsilon})^L$.

Pseudo-count method. In this method, we infer ϵ for all three non-cognate nucleotides in each position, and obtain ϵ for the TF as an average of these $3L$ values. For an arbitrary position j , as before, assume that $i = 4$ has the maximum counts ($b_{4j} > b_{ij}$, $i = 1, 2, 3$). We obtain $\epsilon_{ij} = \log \frac{b_{4j}}{b_{ij}}$ and the mismatch penalty for position j as $\epsilon_j = \frac{1}{3}(\epsilon_{1j} + \epsilon_{2j} + \epsilon_{3j})$. If some entry $b_{kj} = 0$, ϵ_{kj} is undefined. To take care of this, we first add a pseudocount δ to all entries of B and obtain a modified PCM B_δ to infer ϵ . The value of δ reflects the fact that PCMs are empirically constructed from a finite (and often small) number of binding site samples; consequently, zero observed counts does not imply perfect specificity at some site, but rather that the corresponding probability of observing a particular nucleotide is small. Typically, one uses $\delta = 0.5$ or $\delta = 1$. As before, to get rid of non-specific positions, we consider positions that have $\epsilon_j \geq 1$. This is similar to the previous exclusion criterion in the information method; requiring $\epsilon_j \geq 1$ is equivalent to requiring $I_j \geq 0.17$ bits. From the remaining positions, we take a mean to obtain $\epsilon = \frac{1}{L} \sum_j \epsilon_j$, and finally obtain $S(\epsilon, L) = (\frac{1}{4} + \frac{3}{4}e^{-\epsilon})^L$.

H. Cooperative regulation

In the basic model, we assumed that each gene is regulated through a single TF binding site. Some genes, however, employ combinatorial regulation: their expression is determined by the binding of several TFs, possibly of different types, to different binding sites. Here we extend our basic model with cooperative regulation, where every gene has two binding sites that are preferably bound by two copies of the same type of transcription factor.

We assume 2 binding sites per gene, with an energy gap E_a between cognate-bound and unbound states. An additional energy contribution Δ is obtained if both sites are bound by cognate factors, which may interact with each other. We consider also the configuration that two noncognate factors of the same type bind to the double binding sites and interact with each other as well. In the limit that $\Delta \gg E_a$ once one of the sites is bound, the binding of the other becomes energetically favorable. This cooperative binding energy only applies for two molecules of the same type. Thus, if one site is bound by the cognate and the other by a noncognate molecule, cooperative interaction doesn't apply.

We assume that transcription is induced by the occupancy of only one of the two sites. The reasoning for this assumption is that for many bacterial and yeast genes, the activators are thought to work by recruiting the transcriptional machinery to the DNA [13]. Following this rationale, only one of the two sites is in the correct physical location (in bacteria, the proximal one) to do so successfully. Technically, if we assume that only one of the two sites determines transcription, the cooperativity case reduces back to the basic model for $\Delta = 0$ (Section III A). We list

the possible binding configurations of the two sites, their energies, and statistical weights in Table II.

	configuration	activity	crosstalk if ON	crosstalk if OFF	strong cooperativity	Energy	Weight
1	CC	ON	-		+	0	$(C/Q)^2$
2	UC	ON	-			$E_a + \Delta$	$C/Qe^{-E_a - \Delta}$
3	NC	ON	-			$\Delta + \epsilon d$	$C^2/QSe^{-\Delta}$
4	UU	OFF	+	-	+	$2E_a + \Delta$	$e^{-2E_a - \Delta}$
5	CU	OFF	+	-		$E_a + \Delta$	$C/Qe^{-E_a - \Delta}$
6	NU	OFF	+	-		$E_a + \Delta + \epsilon d$	$CSe^{-E_a - \Delta}$
7	UN	*	+	+		$E_a + \Delta + \epsilon d$	$CSe^{-E_a - \Delta}$
8	CN	*	+			$\Delta + \epsilon d$	$C^2/QSe^{-\Delta}$
9	$N_x N_y$	*	+	+		$\Delta + \epsilon(d_1 + d_2)$	$C^2 S^2 e^{-\Delta}$
10	$N_x N_x$	*	+	+	+	$2\epsilon d$	$\frac{C^2}{Q} S(2\epsilon, L)$

TABLE II. All possible binding configurations and the corresponding energies for a model with two binding sites and cooperativity. ‘C’ denotes binding by cognate factor; ‘N’ binding by noncognate factor; ‘U’ means that the site is unbound. We distinguish between binding of noncognate molecules of the same type ($N_x N_x$) and different types ($N_x N_y$), where in the former case there is also cooperative interaction between the molecules. We define the reference energetic level $E = 0$ as the state ‘CC’ when both sites are bound by cognate factors with cooperative interaction, such that all other energies are positive. We assume that the left binding site is distal and only the right one (the proximal site) determines the state of activity. Note that the statistical weight of the last binding configuration $N_x N_x$ uses $S(2\epsilon, L)$ instead of $S(\epsilon, L)$. The column ‘activity’ denotes whether in the given configuration the gene is either ON, OFF or * - could be either active or inactive (possibly active in response to noncognate signal). Blank space denotes a non-existing configuration (or one which is not accounted for): these are the configurations including a cognate factor bound in the situation that it is absent because the gene should be silent. The next two columns denote whether this configuration was counted as crosstalk (+) or not (-) if the cognate transcription factor is present and the gene should be activated or if it is absent (and the gene should be silenced). The ‘Strong Cooperativity’ column denotes that a given configuration is included for the strong cooperativity approximation.

The general solution for this model which incorporates all possible binding configurations yields a 6th order equation for the optimal TF concentration C , which we can only handle numerically. The following limiting cases are however analytically solvable:

1. Limit of strong cooperativity: Assume that the cooperative interaction is strong compared to the individual protein-DNA binding energies $\Delta \gg E_a$. We can then neglect binding configurations in which only one of the sites is bound and the other is vacant, and the ones in which both are bound, but by molecules that do not interact cooperatively. That leaves us with only 3 possible binding configurations: both sites unbound, both bound by cognate TF or both bound by noncognate TF molecules of the same type with cooperative interaction (configurations 1,4 and 10 in Table II). By proper change of variables this case can be reduced back to the basic single-binding-site model. The minimal crosstalk then reads:

$$X_{\text{coop}}^* = \frac{-Q \left(\tilde{S}(M - Q) + 2\sqrt{\tilde{S}(M - Q)} \right)}{M}, \quad (\text{S29})$$

where $\tilde{S} = S(2\epsilon, L)$. This error is achievable with TF concentration

$$C_{\text{coop}}^* = Q \sqrt{\frac{e^{-\Delta - 2E_a} (\tilde{S}(M - Q) - 1)}{\tilde{S} (\tilde{S}Q(M - Q) + M - 2Q) + \sqrt{\tilde{S}(M - Q)}}}. \quad (\text{S30})$$

Since the cooperative binding model allows for a binding site which is twice as long and for a higher total binding energy, the parameters need to be correctly transformed to compare to the 1-site model. If we transform: $\tilde{S} \rightarrow S$ we obtain exactly the same minimal error as in the single-site model. By proper transformation of the energy of the unbound state $\tilde{E}_a = \Delta + 2E_a$ the TF concentration that minimizes the error is a square root of the one we had in the single-site model Eq. (S11). Similarly to the basic single-site model, here too we obtain three different parameter regimes (e.g., for $\tilde{S} = S(2\epsilon, L) > \frac{1}{M-Q}$, the minimal error is obtained by taking $C = 0$, etc.). While the cooperative binding seems completely equivalent to the basic, single-site model whose binding site is double the length, this is not accurate. The reason is that cooperative interaction occurs only between two specific molecules, which limits the possible sequence space.

2. Limit of weak cooperativity: If $\Delta = 0$, the problem reduces to the basic single-site model.

I. Cooperativity with interactions between noncognate pairs

Figure 5 of the main text is computed assuming that cooperative interactions are perfectly specific, i.e., that two TFs that are noncognate to their sites, but of the same type, cannot gain the cooperative benefit Δ ; specifically, configuration 10 from Table II was not included in the calculation. This “specific cooperativity,” as argued in the main text, puts strong requirements on the molecular mechanisms that implement it, and some known molecular mechanisms are unlikely to satisfy those requirements. For example, if TF molecules cooperatively interact in solution and dimerize before binding, it is likely that they could also bind a pair of noncognate sites as a complex. Similarly, cooperativity induced by competition with nucleosomes should be nonspecific as well. In the following we compute the crosstalk under the “nonspecific cooperativity” regime, where we include configuration 10 of Table II. The results are illustrated in Fig S7. The improvement in crosstalk due to cooperativity is now significantly smaller than in the specific cooperativity case.

J. Weak global repressor

Our basic model has considered regulation by activators. Cells however also have repression mechanisms as an additional means of regulation. As a first step to account for that we incorporate in the model one type of an abundant weak global repressor that interacts with all binding sites with sequence-independent low affinity. Nonspecific repression mechanisms such as the nuclear envelope, histones and DNA methylation are thought to mitigate spurious transcription [14]. It was hypothesized that their emergence enabled the genome expansion in the transitions between prokaryotes to eukaryotes and from invertebrates to vertebrates [14]. We include an additional molecule in the model, which is found at concentration C_r and can bind all binding sites equally with energy $0 < E_r < E_a$, namely its binding is more favorable than the unbound state, but not as favorable as the binding of the specific cognate activator at each site. Hence, our intuition was that such a global repressor cannot compete equally with specific binding, but it can reduce erroneous activation due to noncognate binding. The crosstalk expressions now read:

$$x_1^r = \frac{SC + C_r e^{-E_r} + e^{-E_a}}{SC + \frac{C}{Q} + C_r e^{-E_r} + e^{-E_a}} \quad (\text{S31})$$

$$x_2^r = \frac{SC}{SC + C_r e^{-E_r} + e^{-E_a}}. \quad (\text{S32})$$

As before, we minimize the crosstalk with respect to the TF concentration. The optimal concentration is now:

$$C_{GR}^* = -\frac{Q(C_r e^{-E_r} + e^{-E_a}) \left(\sqrt{S(M-Q)} - S(SMQ - Q(SQ+2) + M) \right)}{S(-M(SQ+1)^2 + SQ^2(SQ+3) + Q)}. \quad (\text{S33})$$

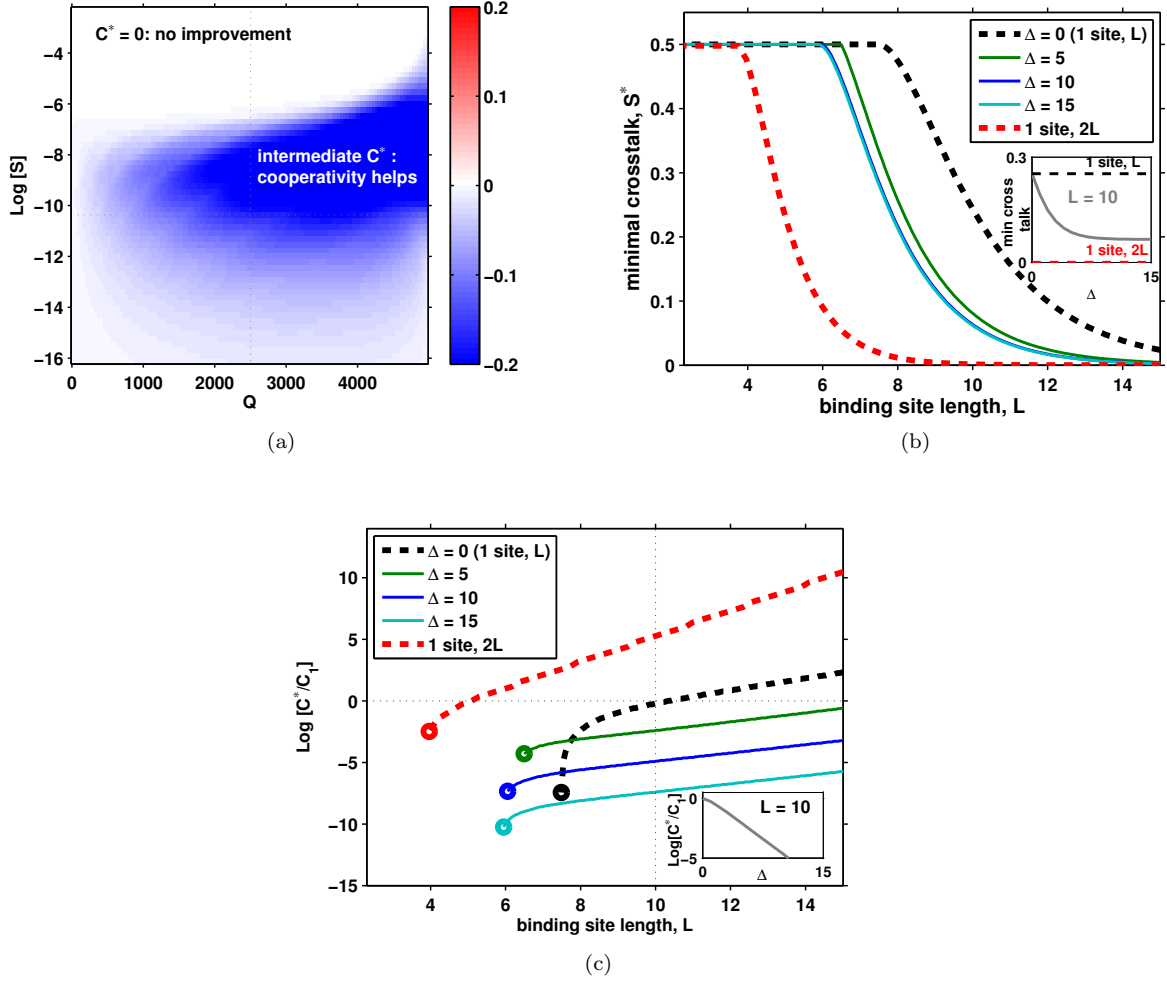


FIG. S7. Minimal crosstalk when any pair of the same-type TFs can interact cooperatively, even if bound to a noncognate site. Here we repeat the calculation of Fig. 5 of the main text but adding in configuration 10 of Table II. This significantly decreases the benefit of cooperative interaction, although it still shows some improvement compared to the single-site basic model. (a): Difference in minimal crosstalk relative to the basic model with a single site, $X_{\text{COOP}}^* - X^*$. The $C^* = 0$ (no regulation regime) becomes significantly larger (compare to Fig. 5B). (b): Minimal crosstalk obtained for different intensities of cooperative interaction. In contrast to the case shown in the main text Fig. 5C, the improvement in crosstalk saturates more quickly at a higher residual level of crosstalk. (c): Optimal TF concentration decreases with increased cooperativity, as in Fig. 5D. Circles denote transition to $C^* = 0$ – the “no regulation” regime.

This is the same optimal concentration C^* as in Eq. (S11) only scaled by a factor $C_r e^{-E_r} + e^{-E_a}$, instead of e^{-E_a} as before. We conclude that the sole effect of a global repressor is to scale down the concentration of the specific activator. This is completely compensated for by a larger optimal concentration of the activator. Hence, regardless of the global repressor affinity E_r and its concentration C_r , this additional regulatory mechanism cannot lower the crosstalk beyond what is possible with specific activators only. As before, the minimal crosstalk is:

$$X_{GR}^* = \frac{Q}{M} \left(-S(M - Q) + 2\sqrt{S(M - Q)} \right). \quad (\text{S34})$$

K. Regulation by a combination of specific activators and specific repressors

As the global repressor examined in the previous section did not show any additional improvement in crosstalk, we elaborate the model further to account for specific repressors, in analogy with the specific activators. We extended the basic model, in which every gene had a single regulatory site for an activating TF, to a more general model, in which

each gene has two regulatory sites: one compatible with a specific activator binding and the other with a specific repressor. We assume that each gene has a unique activator and unique repressor. In the basic model, for a gene to be inactive, its binding site should be vacant. The only way to achieve this was to lower the activator concentration. On the other hand, to improve activation reliability, the activator concentration should be high. Thus, in the simple model there is a trade-off between reliable activation and elimination of undesirable activation. The existence of a specific molecule that blocks the site from binding of other (potentially activating) molecules is thought to be a more reliable way to prevent undesired gene activation, while not obstructing the activation of other genes [15].

To be consistent with the basic model, we assume that the total concentration of all TFs (activators and repressors together) is constant, C . As before, Q genes need to be activated, for which Q specific activators are present. The other $M - Q$ genes need to be inactive, for which we now add $M - Q$ specific repressors. All activators are found in equal concentrations, $C_A/Q = \alpha * C/Q$ for each gene. All repressors are in equal concentrations, $C_R/(M - Q) = (1 - \alpha) * C/(M - Q)$, for each gene. We allow for different binding energies for the two binding sites E_a and E_r . We assume that activation can only occur by binding of an activator molecule to the 'A' site. Repression is asymmetric in the sense that binding of any molecule to the repressor site prevents activation, regardless of what is bound to the activator site. Thus a gene can only be active if the repressor site is empty and the activator site is bound by an activator. See the list of all possible states of the two binding sites in Tables III and IV below.

L. Overlapping activator and repressor binding sites

For some genes, the regulatory sites of the activator and repressor partially overlap. Another possibility is "negative cooperativity" – when one molecule repels the other. The outcome of either option is that either an activator or a repressor could be bound at any given time, but not both of them simultaneously. In Tables III-IV all the states above the double horizontal line are such that only one site can be bound at any given time ('overlapping sites'). The additional states below the line are only possible if both sites can be bound simultaneously ('non-overlapping sites'). Fig S8 illustrates the dependence of crosstalk on the energy E_r (energy gap between unbound and repressor-bound states) for different values of co-activated genes Q . Crosstalk is minimized for $E_r = E_a$ exactly when $Q = M - Q$, meaning equal number of activated and repressed genes. However, for other values of $Q \neq M - Q$, E_r is also not significantly different from E_a .

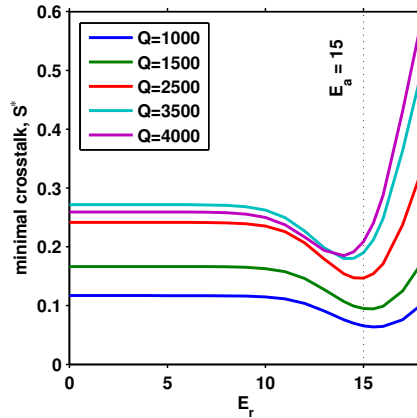


FIG. S8. **Activator-repressor overlapping binding sites, different Q values.** E_r^* – the energy gap between unbound and repressor-bound states – that minimizes crosstalk depends on the number of co-activated genes Q . Here we show numerical results for the minimal crosstalk, X^* , as a function of the repressor binding affinity E_r (with constant activator affinity $E_a = 15$) for different numbers of co-activated genes Q , in the model where activator and repressor binding sites overlap. We find that when the number of co-activated genes decreases (so that more genes need to be repressed) the optimal repressor affinity E_r^* increases, so that repressors more effectively bind their cognate binding sites and eliminate spurious transcription. When the number of genes that need to be activated equals the numbers of genes that need to be repressed, $Q = M - Q$, we obtain that full symmetry between activator and repressor, $E_r^* = E_a$, provides minimal crosstalk – this case is shown in the main text, Fig. 6. Parameters: $M = 5000$, $S = 10^{-4.5}$.

	configuration (R-site,A-site)	activity	crosstalk if ON	Energy	Weight
1	U, U	OFF	+	$E_a + E_r$	$e^{-(E_a+E_r)}$
2	U, C_A	ON	-	E_r	$\frac{C}{Q}\alpha e^{-E_r}$
3	U, N_A	*	+	$E_r + \epsilon d$	$C\alpha S e^{-E_r}$
4	U, N_R	OFF	+	$E_r + \epsilon d$	$C(1 - \alpha)S e^{-E_r}$
5	C_A , U	OFF	+	$E_a + \epsilon d$	$\frac{C}{Q}\alpha S e^{-E_a}$
6	N_A , U	OFF	+	$E_a + \epsilon d$	$C\frac{Q-1}{Q}\alpha S e^{-E_a}$
7	N_R , U	OFF	+	$E_a + \epsilon d$	$C(1 - \alpha)S e^{-E_a}$
8	$(N_A, C_A), C_A$	OFF	+	ϵd	$\frac{(C\alpha)^2}{Q} S$
9	C_A, N_A	OFF	+	$\epsilon(d_1 + d_2)$	$\frac{(C\alpha)^2}{Q} S^2 \frac{Q-1}{Q}$
10	N_R, C_A	OFF	+	ϵd	$\frac{C^2}{Q} S\alpha(1 - \alpha)$
11	$(N_A, N_R), N_A$	OFF	+	$\epsilon(d_1 + d_2)$	$C^2 S^2 \alpha \frac{Q-1}{Q} \frac{Q-\alpha}{Q}$
12	$(N_R, N_A, C_A), N_R$	OFF	+	$\epsilon(d_1 + d_2)$	$C^2 S^2 (1 - \alpha)$

TABLE III. **All possible binding configurations, corresponding energies, and statistical weights for a two-binding-site (A,R)-model in case a gene needs to be activated.** For a gene that needs to be activated, its cognate activator is present and its cognate repressor is absent. The subscripts ‘A’ and ‘R’ refer to activator and repressor. We assume that the site to which the molecule binds determines the activity state, where binding to an A-site can activate the gene and binding to the R-site (even if it is an activator) hinders activation. ‘C’ denotes binding by a cognate factor, ‘N’ binding by a noncognate factor, and ‘U’ that the site is unbound. E_a and E_r are the energy gaps between unbound and cognate-bound states of the corresponding binding sites. In the upper part of the table (above the double line) we enumerate only states that are possible when both sites cannot be bound simultaneously (‘overlapping sites’ model). If the two sites can be bound simultaneously, there are additional binding configurations, which are enumerated below the line. The column ‘crosstalk if ON’ lists all binding configurations that were accounted for as crosstalk in x_1 calculation – in this case all except for configuration 2 (U, C_A).

-
- [1] P. H. Von Hippel and O. G. Berg. On the specificity of DNA-protein interactions. *Proceedings of the National Academy of Sciences*, 83(6):1608, 1986.
- [2] Ulrich Gerland, J. David Moroz, and Terence Hwa. Physical constraints and functional characteristics of transcription factor-DNA interaction. *Proceedings of the National Academy of Sciences*, 99(19):12015–12020, 2002.
- [3] Franz M. Weinert, Robert C. Brewster, Mattias Rydenfelt, Rob Phillips, and Willem K. Kegel. Scaling of Gene Expression with Transcription-Factor Fugacity. *Physical Review Letters*, 113(25):258101, December 2014.
- [4] Margaret E. Johnson and Gerhard Hummer. Evolutionary Pressure on the Topology of Protein Interface Interaction Networks. *The Journal of Physical Chemistry B*, 117(42):13098–13106, October 2013.
- [5] E. Nimwegen. Scaling laws in the functional content of genomes. *Trends Genet*, 19:479–84, 2003.
- [6] Sebastian J. Maerkl and Stephen R. Quake. A Systems Approach to Measuring the Binding Energy Landscapes of Transcription Factors. *Science*, 315(5809):233–237, January 2007.
- [7] S. Gama-Castro, H. Salgado, M. Peralta-Gil, A. Santos-Zavaleta, L. Muiz-Rascado, H. Solano-Lira, V. Jimenez-Jacinto, V. Weiss, J. S. Garca-Sotelo, A. Lopez-Fuentes, et al. RegulonDB version 7.0: transcriptional regulation of Escherichia coli K-12 integrated within genetic sensory

	configuration (R-site,A-site)	activity	crosstalk if OFF	Energy	Weight
1	U, U	OFF	-	$E_a + E_r$	$e^{-(E_a+E_r)}$
2	C_R , U	OFF	-	E_a	$\frac{C(1-\alpha)}{M-Q} e^{-E_a}$
3	N_A , U	OFF	-	$E_r + \epsilon d$	$CS\alpha e^{-E_a}$
4	N_R , U	OFF	-	$E_r + \epsilon d$	$CS(1-\alpha)e^{-E_a}$
5	U, N_A	*	+	$E_a + \epsilon d$	$CS\alpha e^{-E_r}$
6	U, (C_R , N_R)	OFF	-	$E_a + \epsilon d$	$CS(1-\alpha)e^{-E_r}$
7	C_R , (C_R N_R , N_A)	OFF	-	$E_a + \epsilon d$	$\frac{C(1-\alpha)}{M-Q} CS$
8	N_R , (C_R N_R , N_A)	OFF	-	ϵd	$C^2 S^2 (1-\alpha^2)$
9	N_A , (C_R N_R)	OFF	-	$\epsilon(d_1 + d_2)$	$C^2 S^2 (1-\alpha^2)$
10	N_A , N_A	OFF	-	ϵd	$C^2 S^2 \alpha^2$

TABLE IV. **All possible binding configurations, corresponding energies, and statistical weights for a two-binding-site (A,R)-model in case a gene needs to remain inactivated.** A gene that needs to be inactive, its cognate repressor is present and its cognate activator is absent. All notation is the same as in Table III. The column ‘crosstalk if OFF’ lists binding configurations that were accounted for as crosstalk in x_2 calculation – in this case only configuration 5.

response units (Gensor Units). *Nucleic Acids Research*, 39(suppl 1):D98–D105, 2011.

- [8] Anthony Mathelier, Xiaobei Zhao, Allen W. Zhang, Francois Parcy, Rebecca Worsley-Hunt, David J. Arenillas, Sorana Buchman, Chih-yu Chen, Alice Chou, Hans Ienasescu, Jonathan Lim, Casper Shyr, Ge Tan, Michelle Zhou, Boris Lenhard, Albin Sandelin, and Wyeth W. Wasserman. JASPAR 2014: an extensively expanded and updated open-access database of transcription factor binding profiles. *Nucleic Acids Research*, page gkt997, November 2013.
- [9] Aaron T. Spivak and Gary D. Stormo. ScerTF: a comprehensive database of benchmarked position weight matrices for *Saccharomyces* species. *Nucleic Acids Research*, 40(D1):D162–D168, January 2012.
- [10] Zeba Wunderlich and Leonid A. Mirny. Different gene regulation strategies revealed by analysis of binding motifs. *Trends in Genetics*, 25(10):434–440, October 2009.
- [11] Thomas D. Schneider, Gary D. Stormo, Larry Gold, and Andrzej Ehrenfeucht. Information content of binding sites on nucleotide sequences. *Journal of Molecular Biology*, 188(3):415–431, April 1986.
- [12] Otto G. Berg and Peter H. von Hippel. Selection of DNA binding sites by regulatory proteins: Statistical-mechanical theory and application to operators and promoters. *Journal of Molecular Biology*, 193(4):723–743, February 1987.
- [13] Mark Ptashne and Alexander Gann. Transcriptional activation by recruitment. *Nature*, 386(6625):569–577, 1997.
- [14] Adrian P. Bird. Gene number, noise reduction and biological complexity. *Trends in Genetics*, 11(3):94–100, March 1995.
- [15] Guy Shinar, Erez Dekel, Tsvi Tlusty, and Uri Alon. Rules for biological regulation based on error minimization. *Proceedings of the National Academy of Sciences of the United States of America*, 103(11):3999–4004, March 2006.